Fermi surface topology and chirality in Weyl semimetals

Elena Hassinger

Max Planck Institute for Chemical Physics of Solids

TU München

MPI Chemical Physics of Solids, Dresden

Collaborators

Frank Arnold
Marcel Naumann

Quantum oscillations

Theory support

Adolfo G. Grushin
Jens H. Bardarson

Ricardo Donizeth dos Reis
Chandra Shekhar
Nitesh Kumar

resistivity

M.O. Ajeesh
Binghai Yan
Shu-Chun Wu

Band structure

Yan Sun

Magnetization

Michael Baenitz
Marcus Schmidt
Horst Borrmann

Samples + orientation

Dmitry Sokolov
Michael Nicklas
Claudia Felser

Max-Planck Institute
For Physics of Complex Systems

Max-Planck Institute for

Outline

- Fermi surface of TaP
- Negative longitudinal magnetoresistance
- Fermi surface of TaAs, chirality and Berry phase

Weyl fermions - relativistic particles

fundamental particles
Massless (= gapless) solution of Dirac equation

Hermann Weyl
1929

$$H = \pm v\vec{\sigma} \cdot \vec{k}$$

Chirality

Linear dispersion

Dirac versus Weyl semimetals

Linear dispersion from band crossing

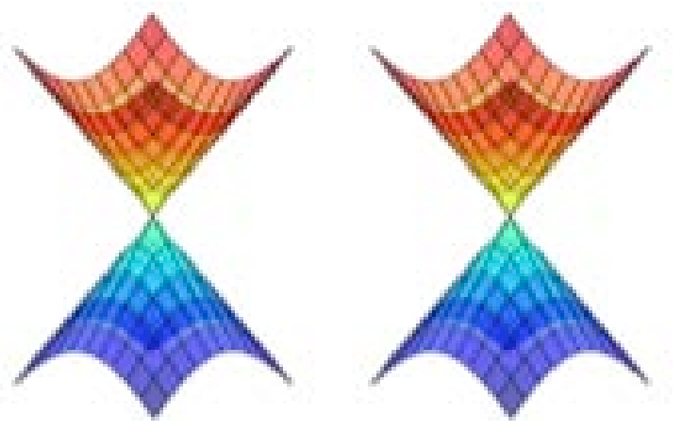

Dirac cone in 3D

$$H = \pm v\vec{\sigma} \cdot \vec{k}$$

Dirac semimetals: Degenerate 3D Dirac cones

Weyl semimetals: Non-degenerate 3D Dirac cone

Weyl semimetals – spin structure

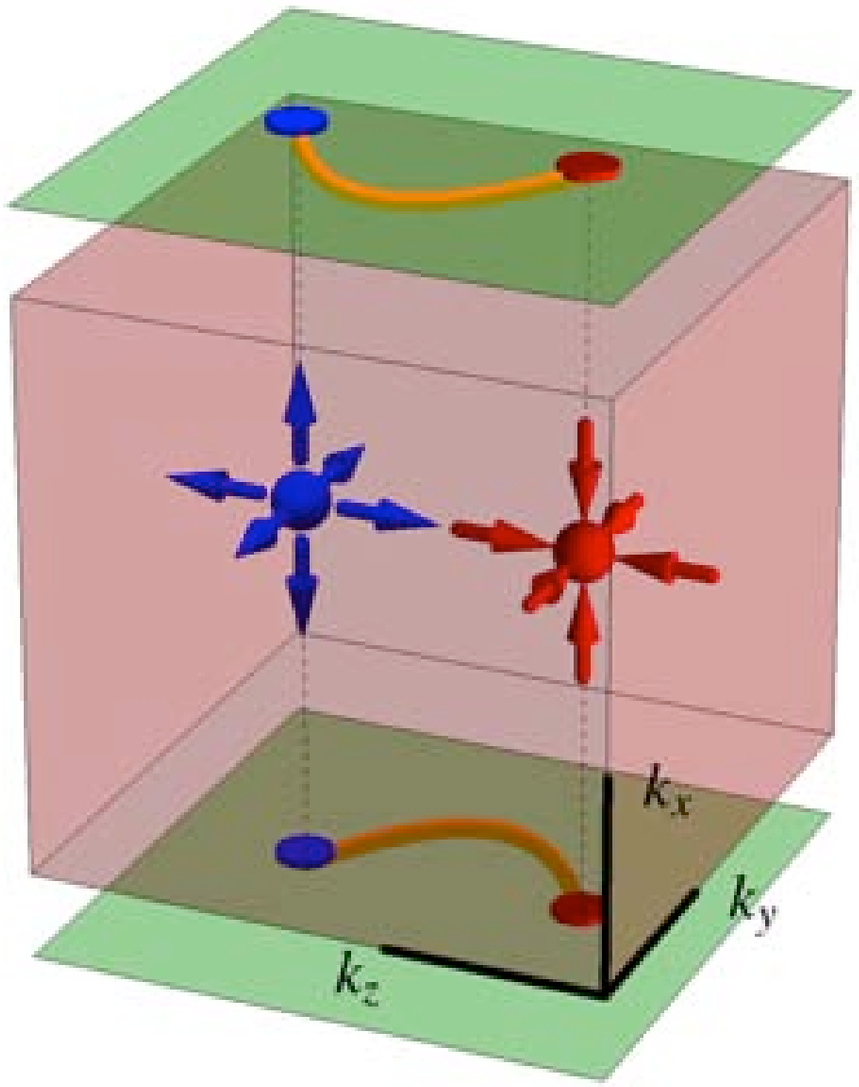

$$H = \pm v\vec{\sigma} \cdot \vec{k}$$

Chirality from spin structure

Magnetic monopoles in k-space
(Source or drain of Berry curvature)
Always come in pairs

Strong spin-orbit coupling required

Volovik, The Universe in a Helium Droplet (2007)
Murakami, New J. Phys. 9, 356 (2007)

Weyl semimetals – experimental signature

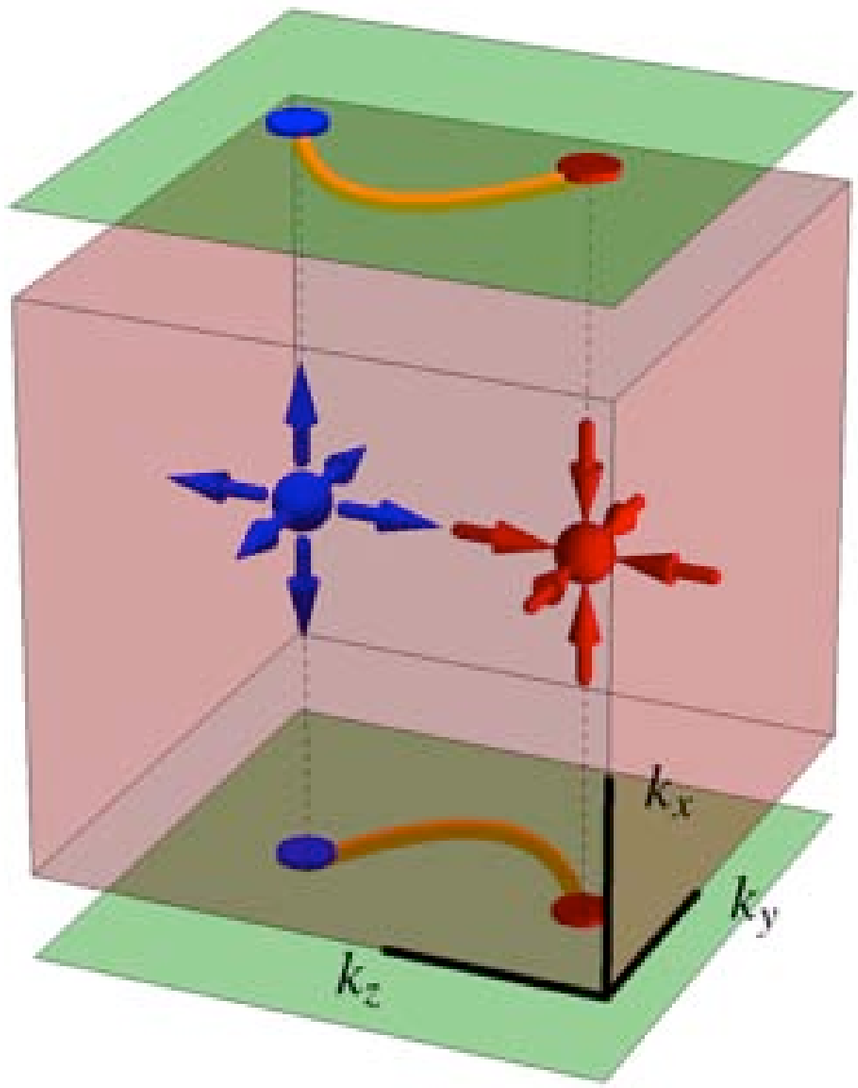

Fermi arc surface states

Detected in ARPES

Reference	material
B. Q. Lv et al., PRX (2015)	TaAs
S. Y. Xu et al., Science (2015)	TaAs
L. X. Yang et al., Nat. Phys. (2015)	TaAs
S. Y. Xu et al., Sci. Adv. (2015)	TaP
S. Y. Xu et al., Nat. Phys. (2015)	NbAs
B. Q. Lv et al., Nat. Phys. (2015)	TaAs
D. F. Xu et al., Chin. Phys. Lett. (2015)	NbP
N. Xu et al., Nat Comm. (2016)	TaP
Z. K. Liu et al., Nat. Mat. (2016)	all 4

Weyl semimetals – experimental signature

chiral anomaly

Adler-Bell-Jackiw anomaly
Axial anomaly
Leads to negative longitudinal magnetoresistance

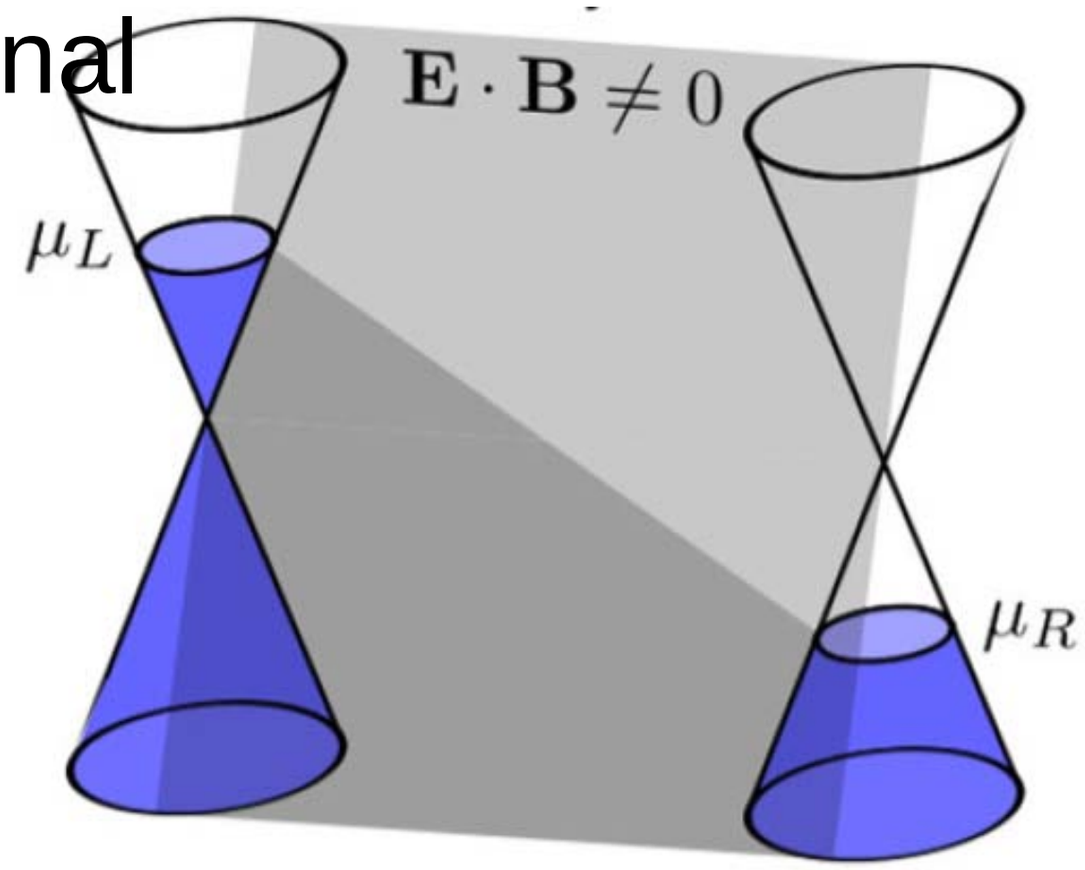

S. Adler, Phys. Rev. 177, 2426 (1969).
J. S. Bell and R. A. Jackiw, Nuovo Cimento A 60, 47 (1969).
H. B. Nielsen and M. Ninomiya, Phys. Lett. B 130, 389 (1983). [negative MR in crystal]
Wan, Tuner, Vishwanath, PRB 2011
Burkov, Hook Balents, PRB 2011
Son, Spivak, PRB 2013
Parameswaran et al. PRX 2014
Hosur and Qi, Comp. Rend. Phys. 2013

Negative longitudinal magnetoresistance

$TaAs_2$ (not a Weyl semimetal)

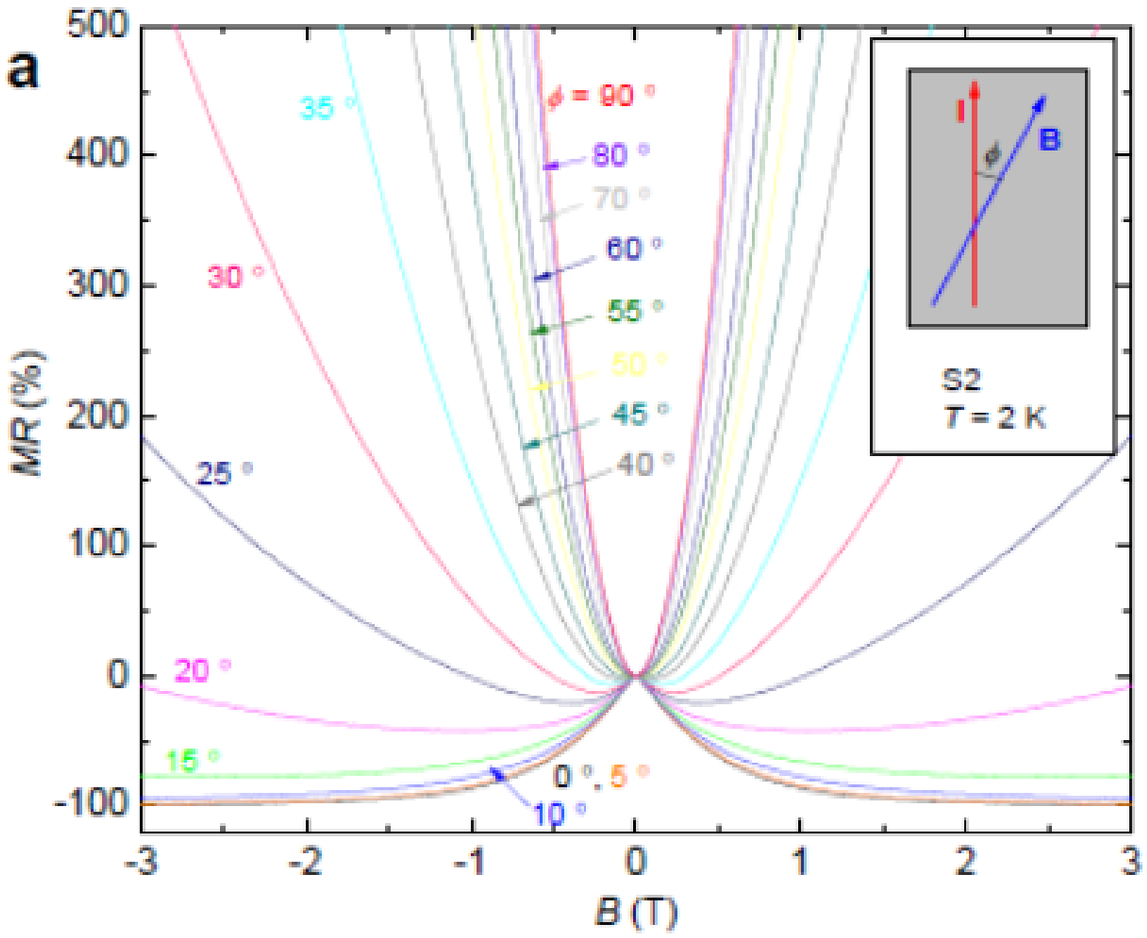

$$MR = (\rho - \rho_0) / \rho_0$$

Luo et al., Scientific Reports (2016)

$$\sigma_a = \frac{e^3 v_f^3}{4\pi^2 \hbar \mu^2 c} B^2$$

Reference	material
X. C. Huang et al., PRX (2015)	TaAs
C. L. Zhang et al., Nat. Comm (2015)	TaAs
X. J. Yang et al., arxiv (2015)	NbAs
J. H. Du et al., Sci. China-Phys. (2015)	TaP
Z. Wang et al., PRB (2015)	NbP
J. Xiong et al., Science (2015)	Na_3Bi
G. L. Zheng et al., PRB (2015)	$ZrTe_5$

Normal versus Weyl semimetals

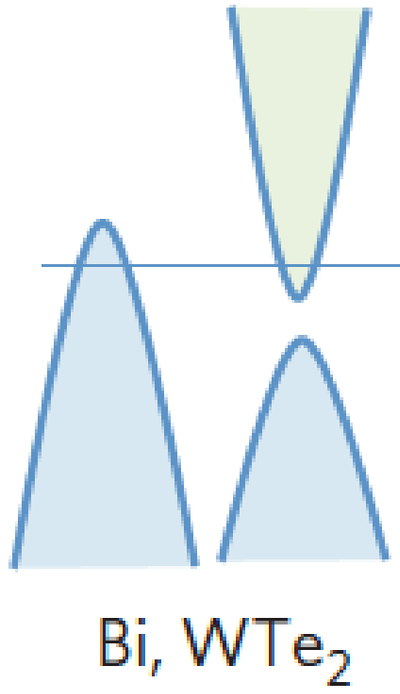

Bi, WTe_2

Normal semimetal

Low carrier density
Small effective masses ($0.01m_0$)
High mobility
Compensated systems

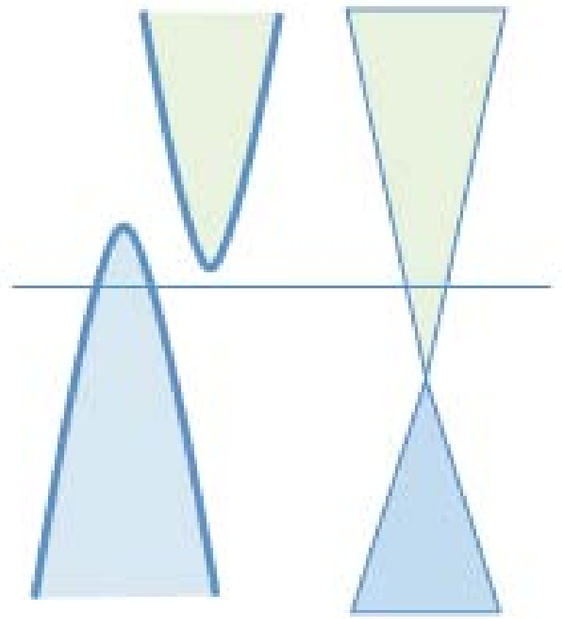

NbP

Weyl semimetal

Weyl nodes near Fermi energy

Shekhar et al. Nat. Phys. 2015

Normal versus Weyl semimetals

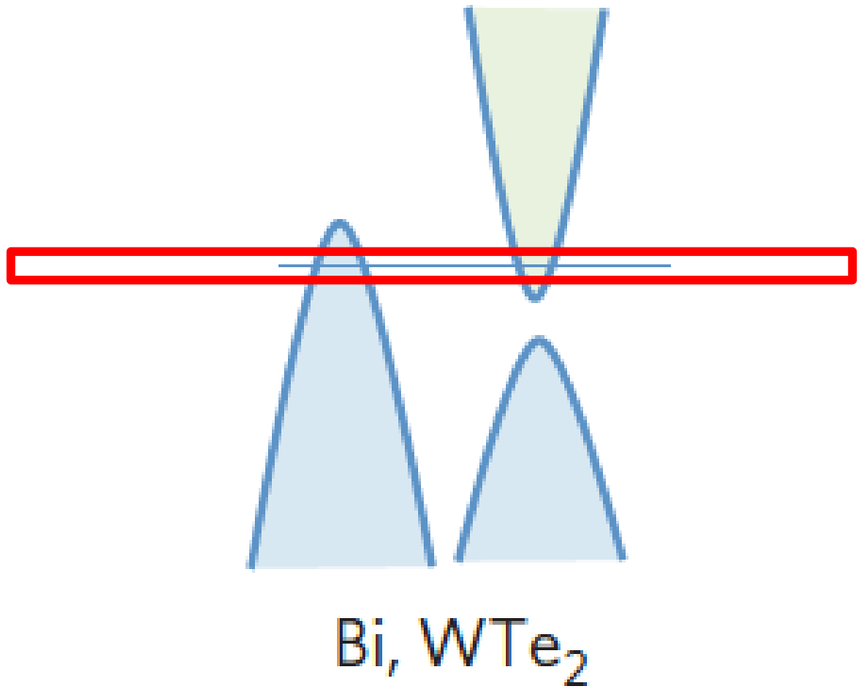

Normal semimetal

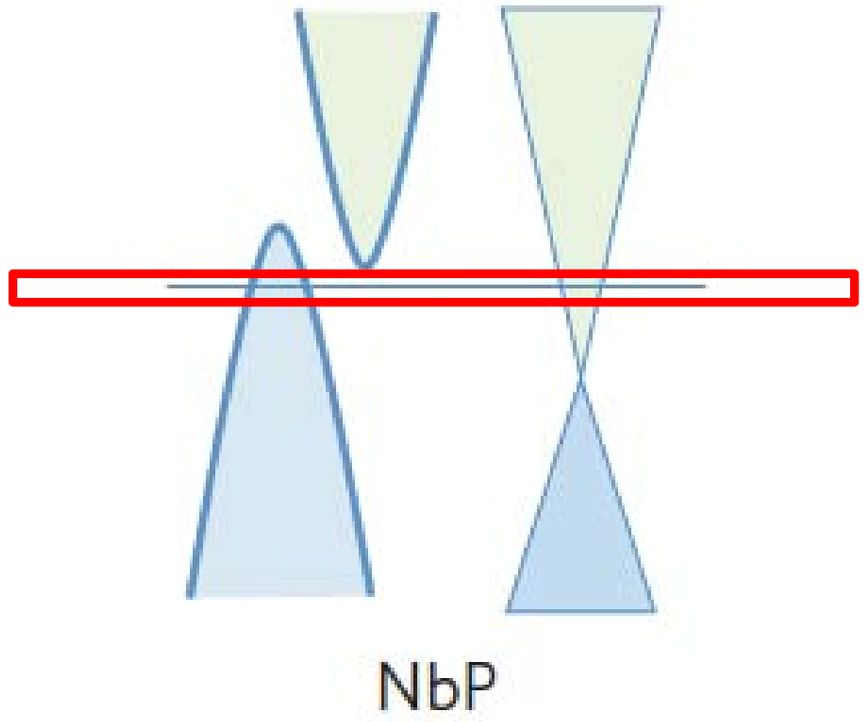

Weyl semimetal

How far are Weyl nodes from E_F?
Do we expect to see experimental bulk signatures of them?

NbP, NbAs, TaP, TaAs
Predicted topological Weyl semimetals

Tetragonal without inversion symmetry

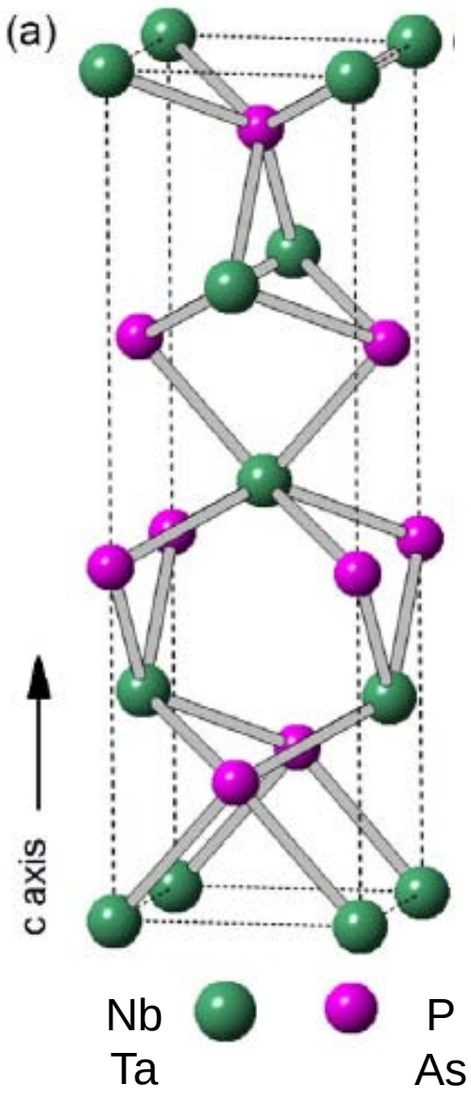

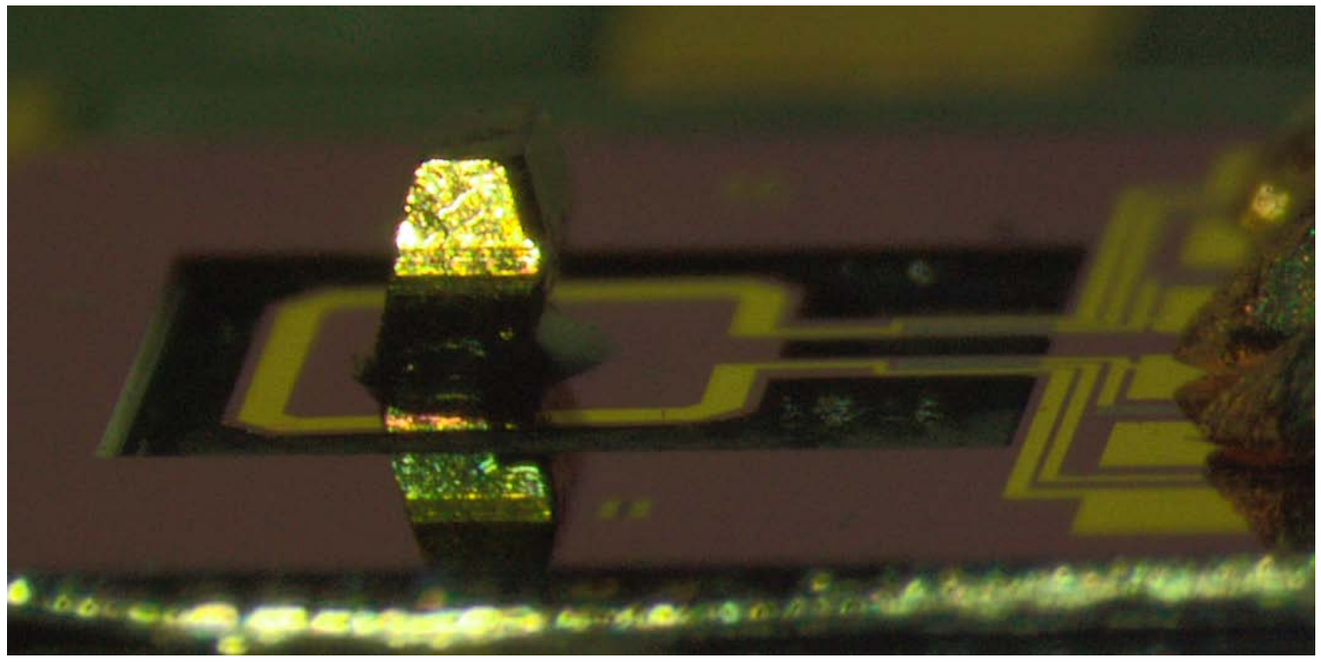

$I4_1md$

Ghimire *et al.* JPCM, 2015

Chiral massless fermions in TaAs semime

Strong spin-orbit coupling,
broken inversion symmetry

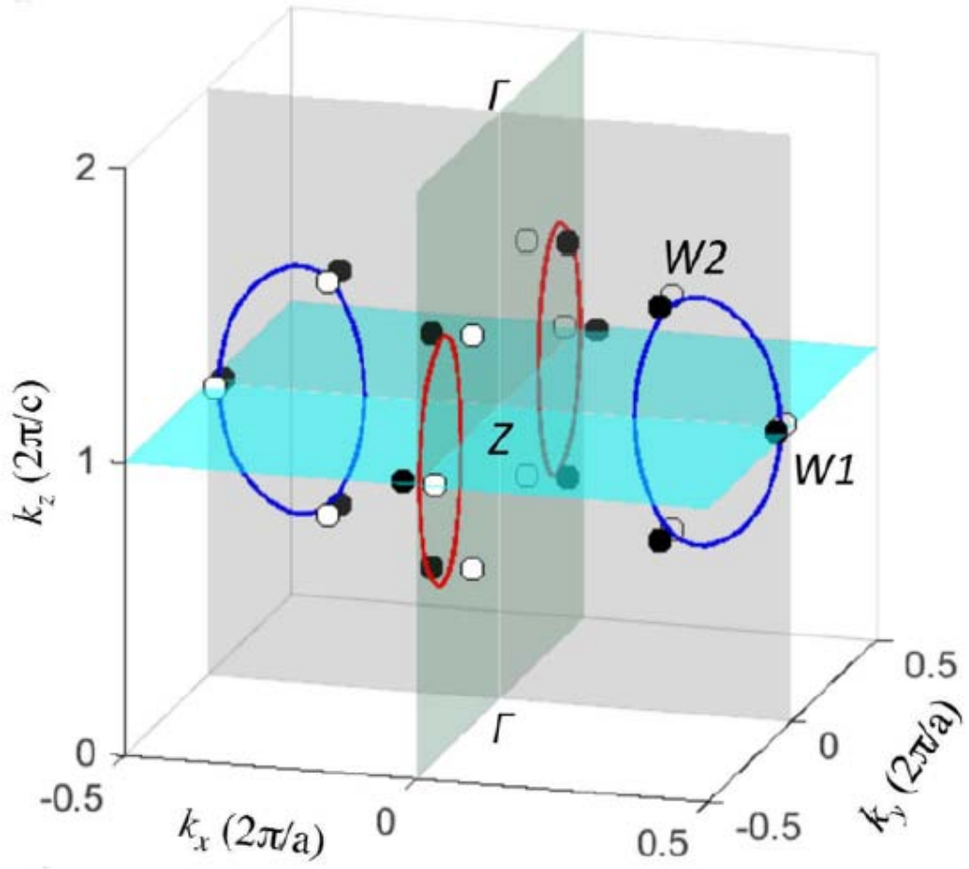

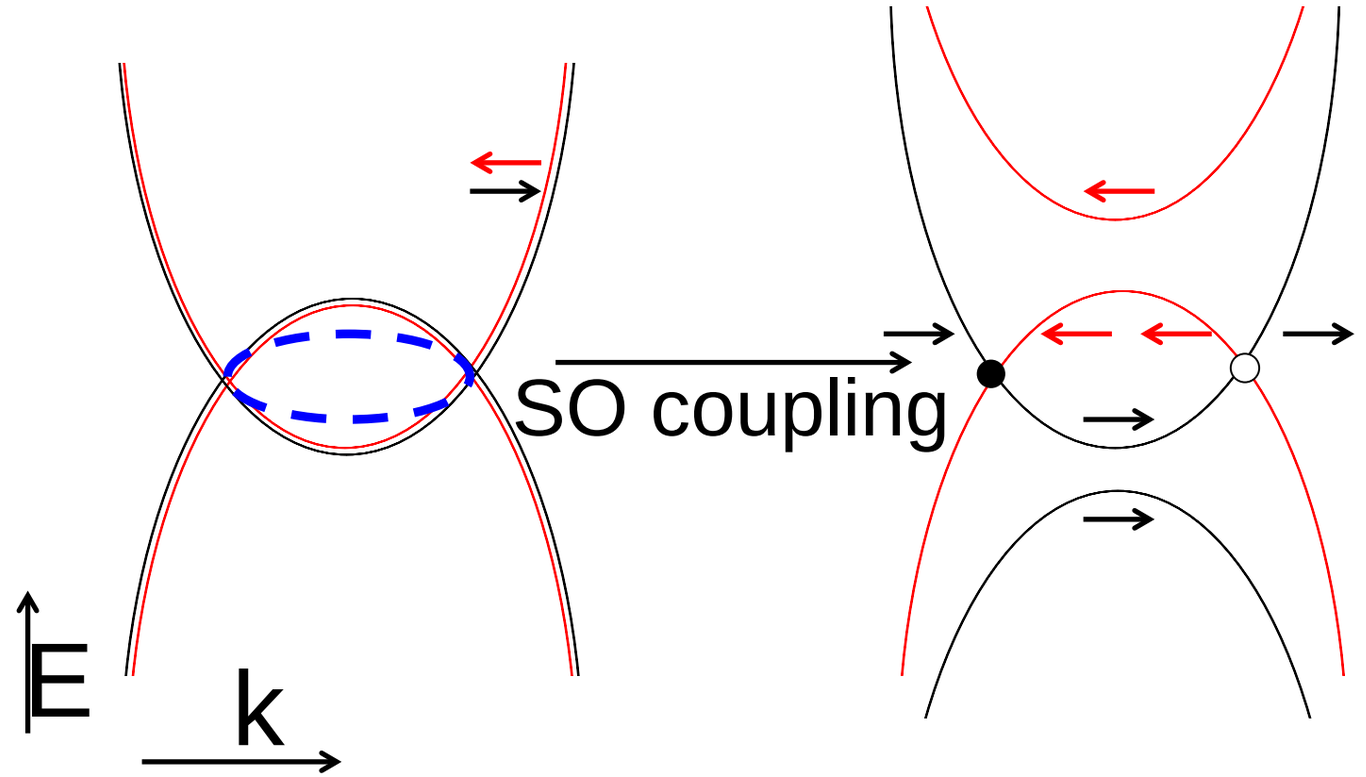

Without SO coupling
Band inversion
Nodal rings

Pairs of band crossing points
opposite chirality

Weng *et al.* PRX, 2015
Huang et al. Nat. Com. 2015

Chiral massless fermions in TaAs semime

Strong spin-orbit coupling,
broken inversion symmetry

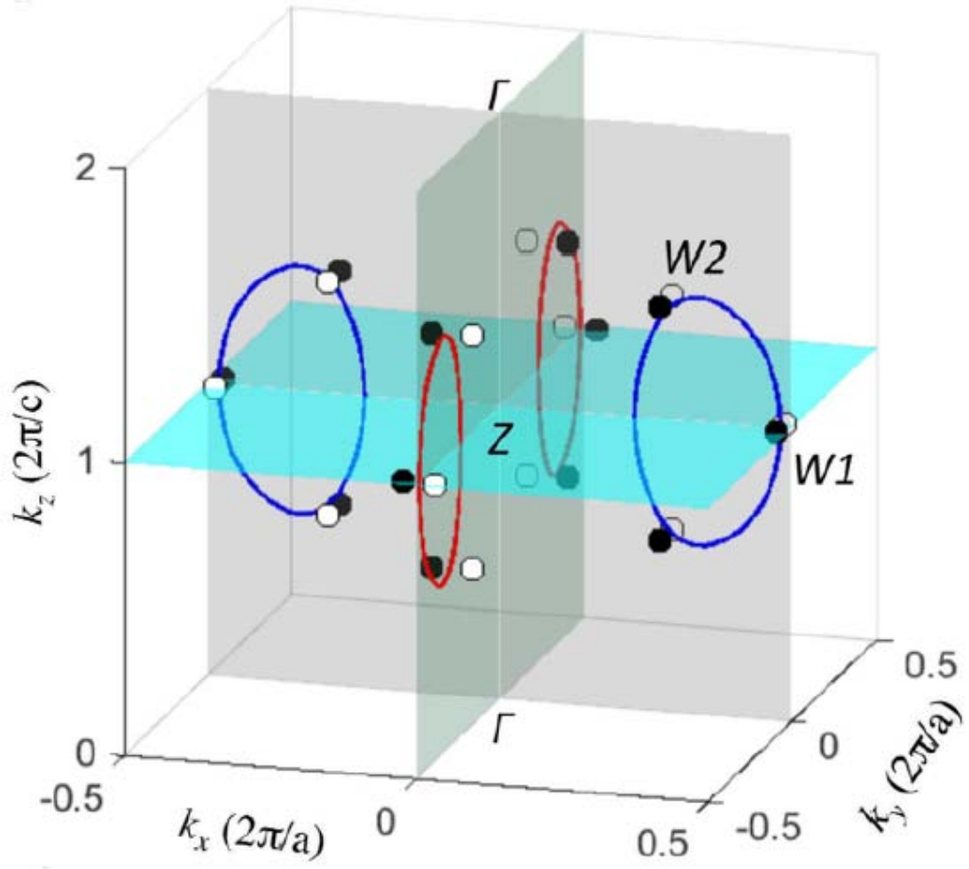

Weng *et al.* PRX, 2015
Huang et al. Nat. Com. 2015

Fermi surface

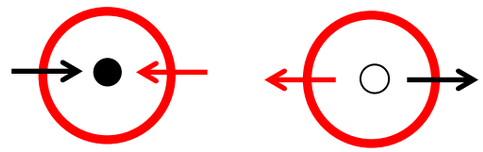

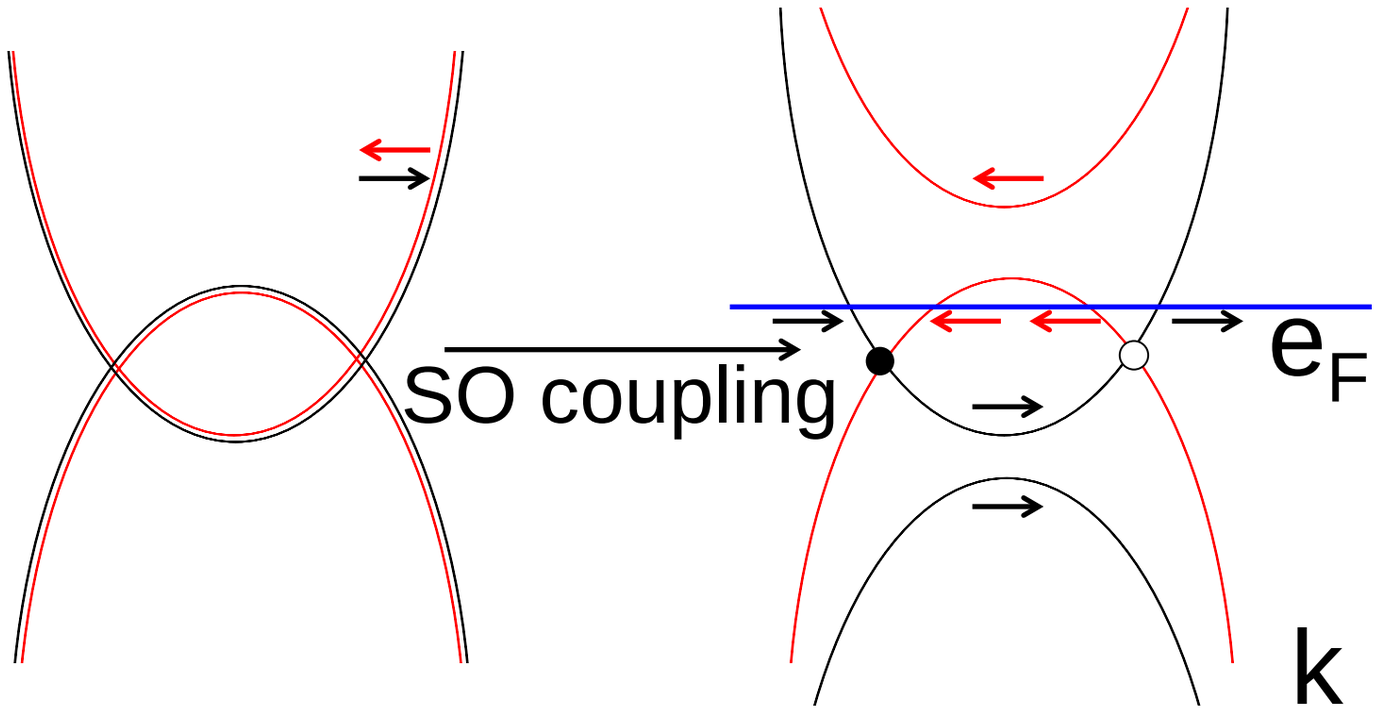

Without SO coupling
Band inversion
Nodal rings

Well-defined
chirality

Chiral massless fermions in TaAs semime

Strong spin-orbit coupling,
broken inversion symmetry

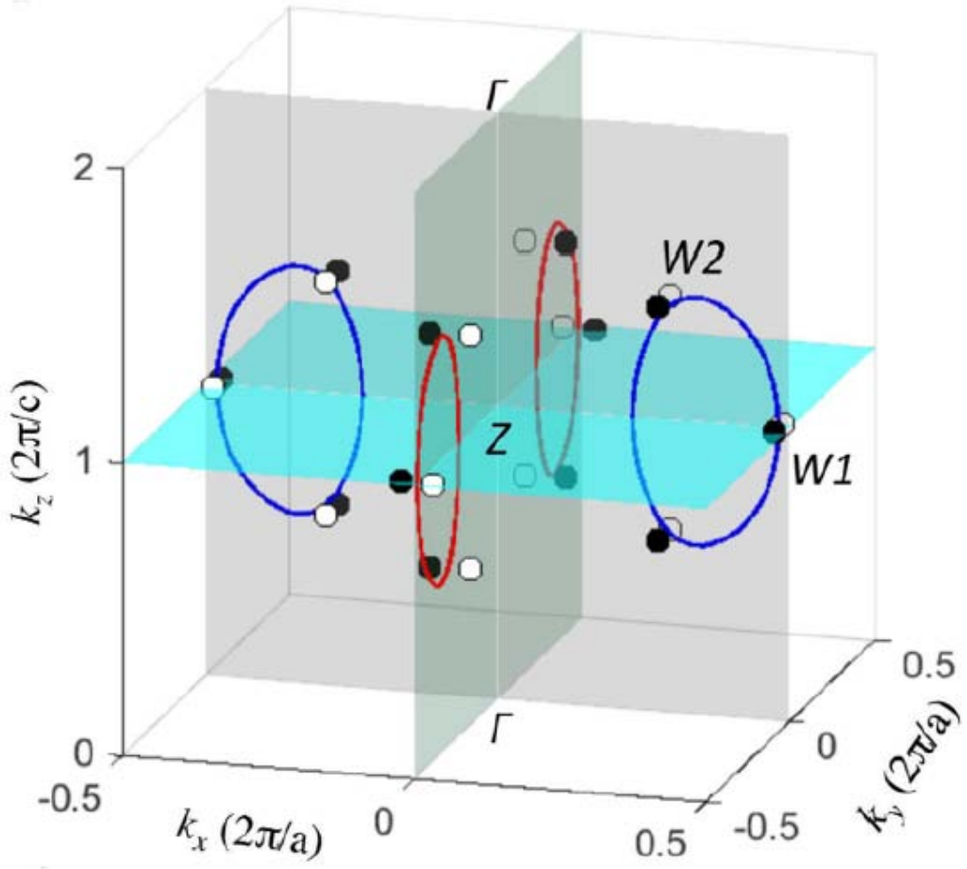

Weng *et al.* PRX, 2015
Huang et al. Nat. Com. 2015

Fermi surface

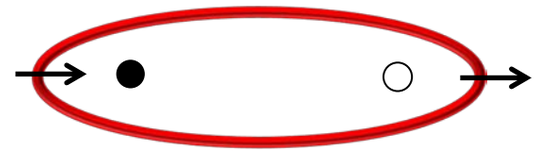

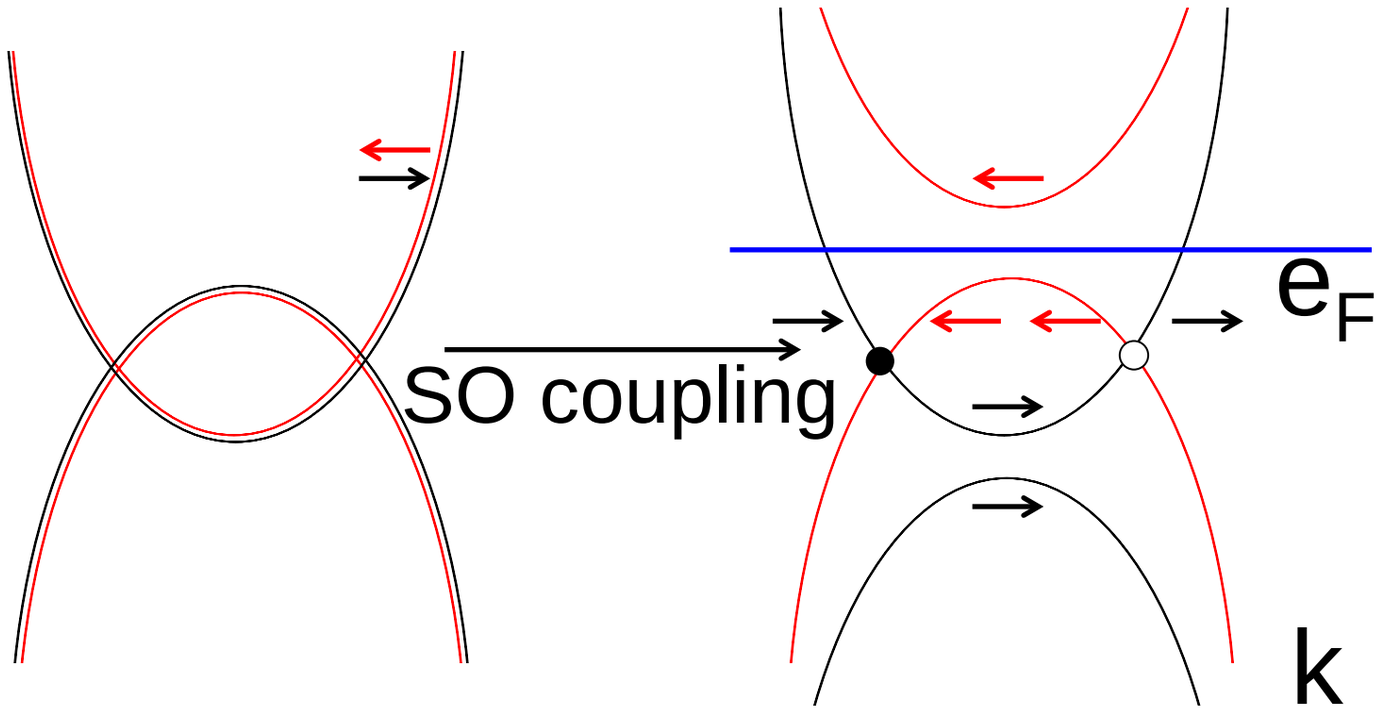

Without SO coupling
Band inversion
Nodal rings

ill-defined chirality

Is the Fermi energy close to the Weyl poin

Two types of Weyl points

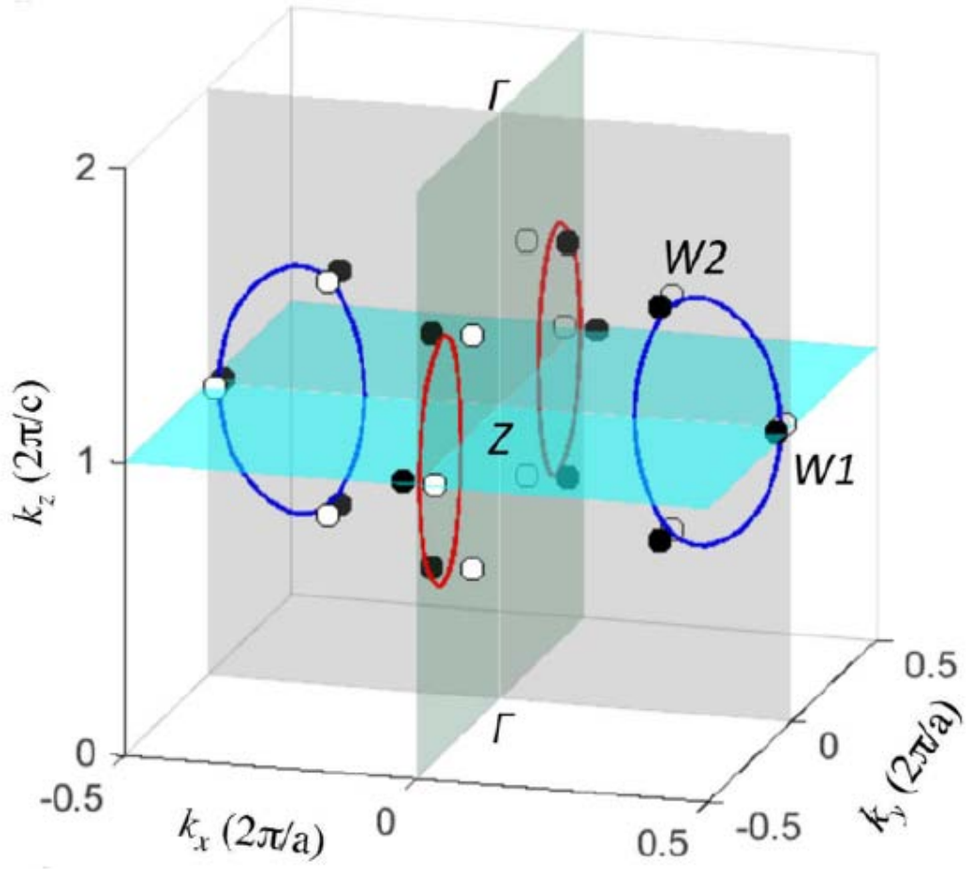

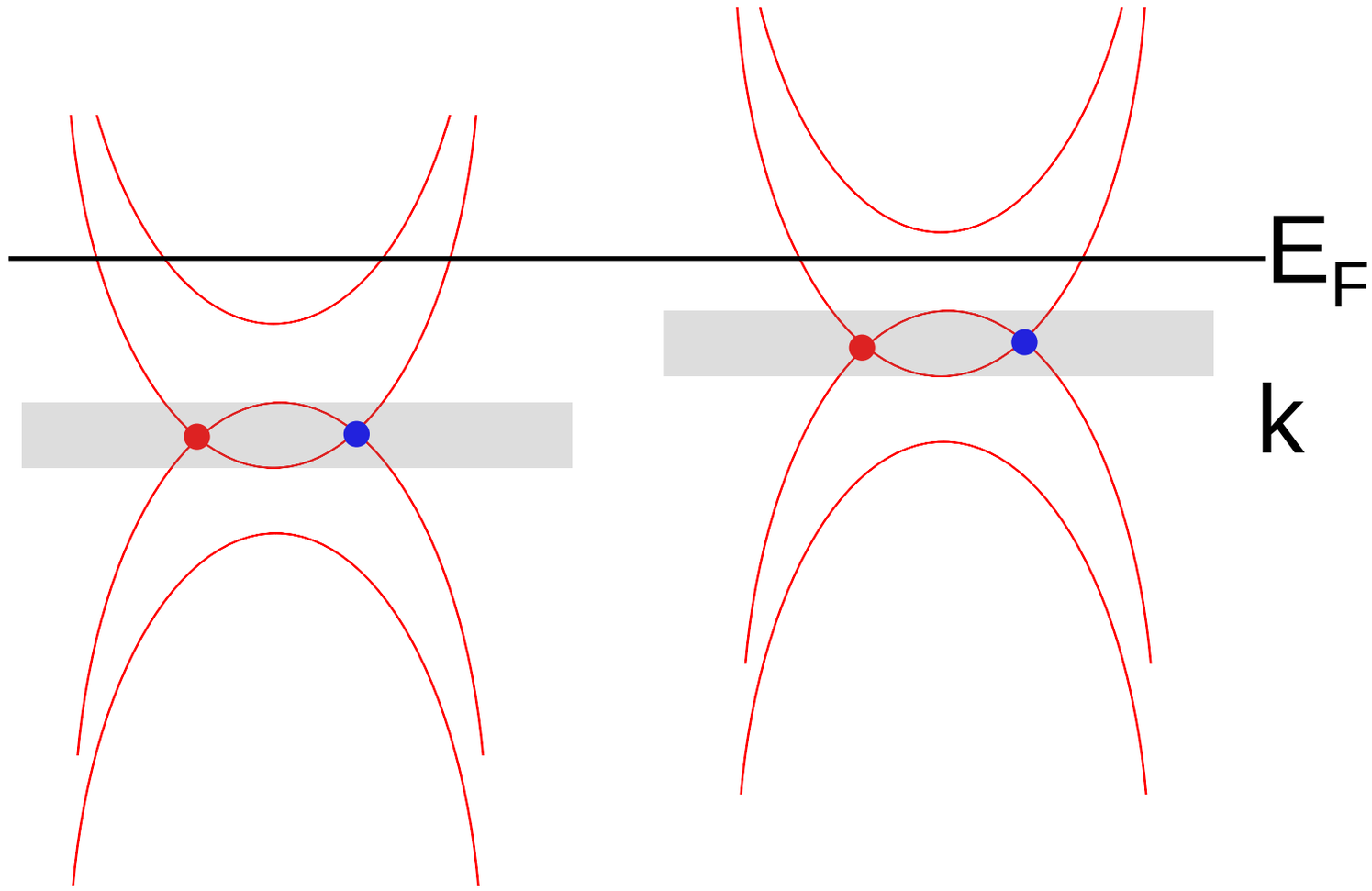

W1

W2

Weng *et al.* PRX, 2015
Huang et al. Nat. Com. 2015

TaP: Magnetization oscillations

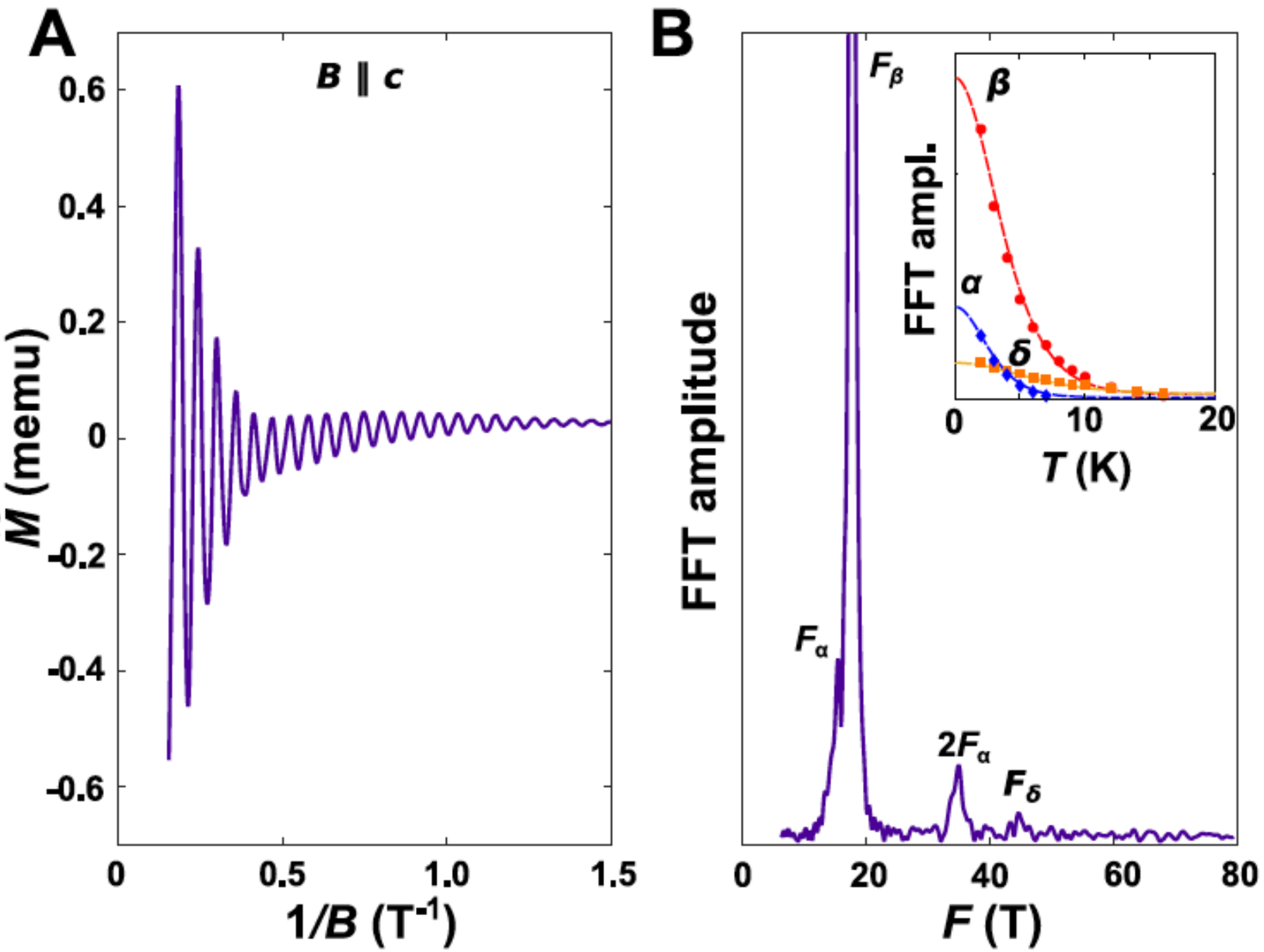

High quality single crystals
Small frequencies
17 T and 45 T

Electron
m* = 0.1

Hole
m* = 0.02

Mobility 3 x10^4 cm^2/Vs = 3 T^{-1}

Mean free path l = 0.4 μm

Quantum oscillations – angular dependence

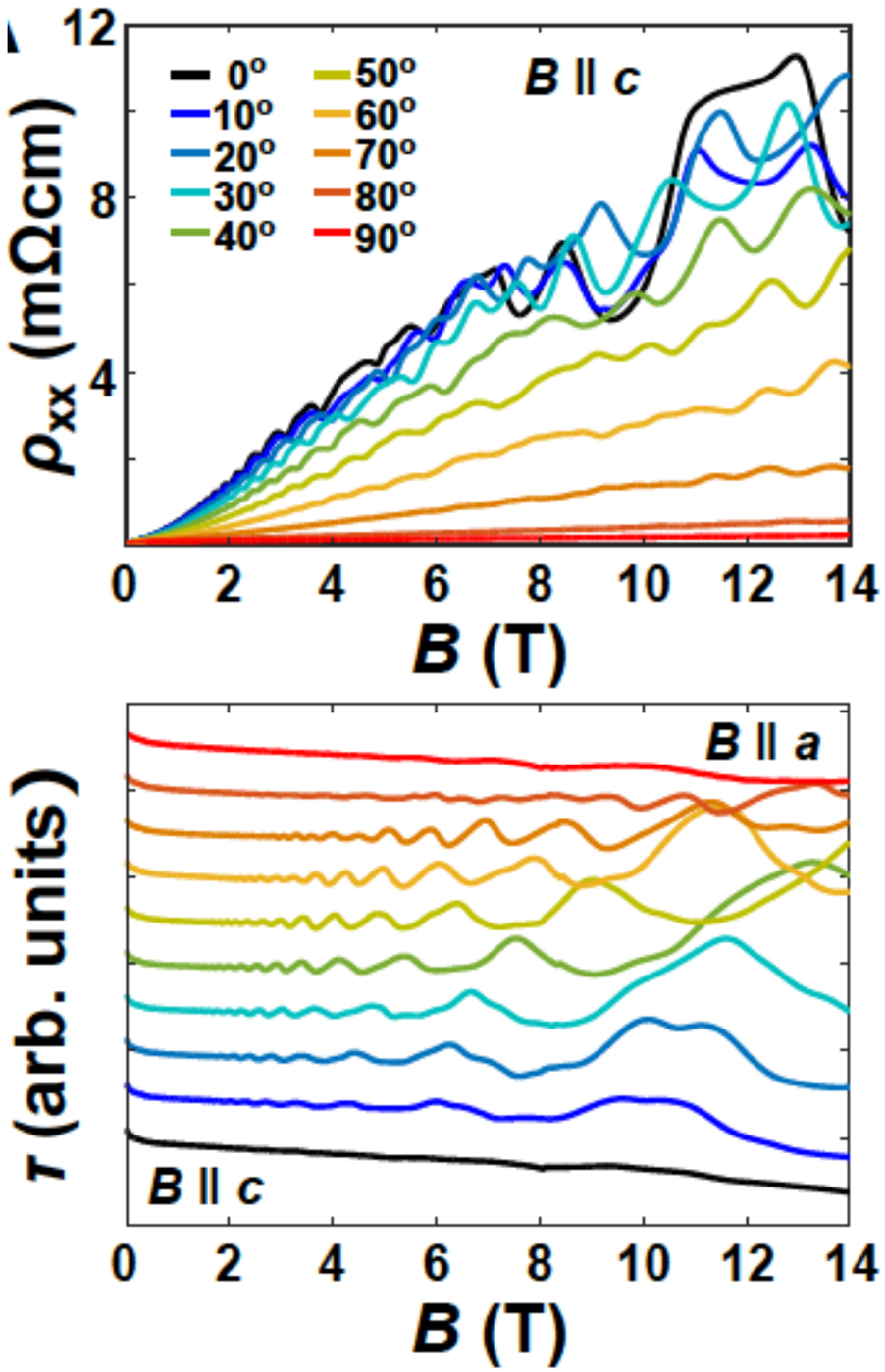

TaP - Bulk Fermi surface

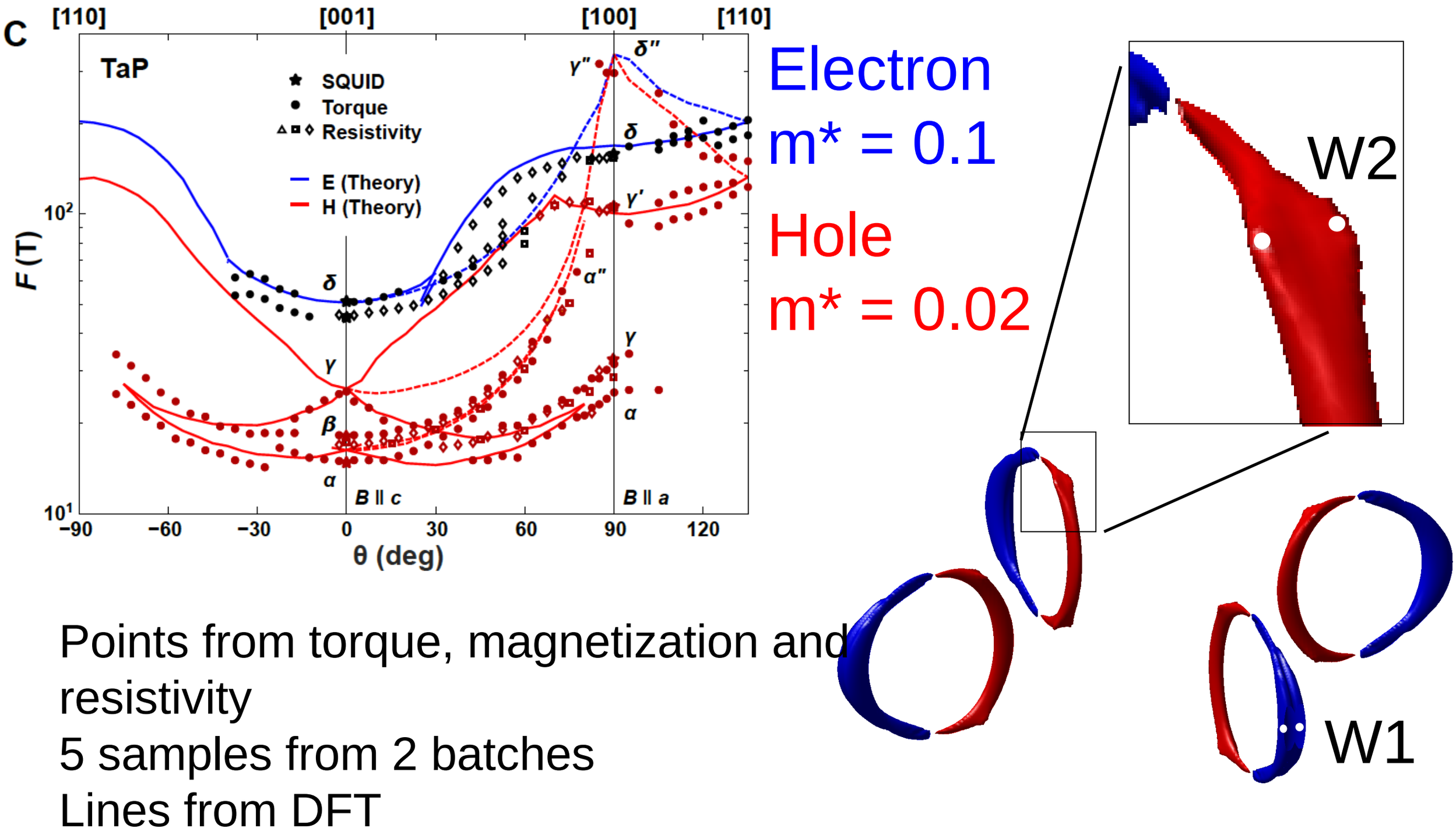

Electron
m* = 0.1

Hole
m* = 0.02

Points from torque, magnetization and resistivity
5 samples from 2 batches
Lines from DFT

Fermi surface topology

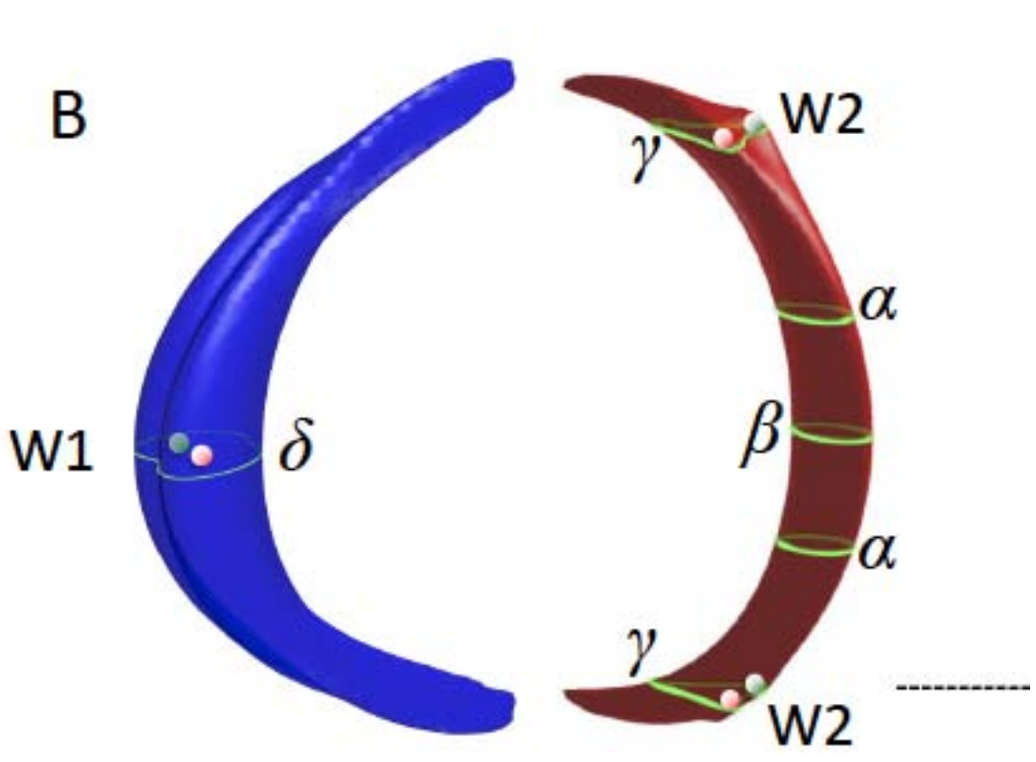

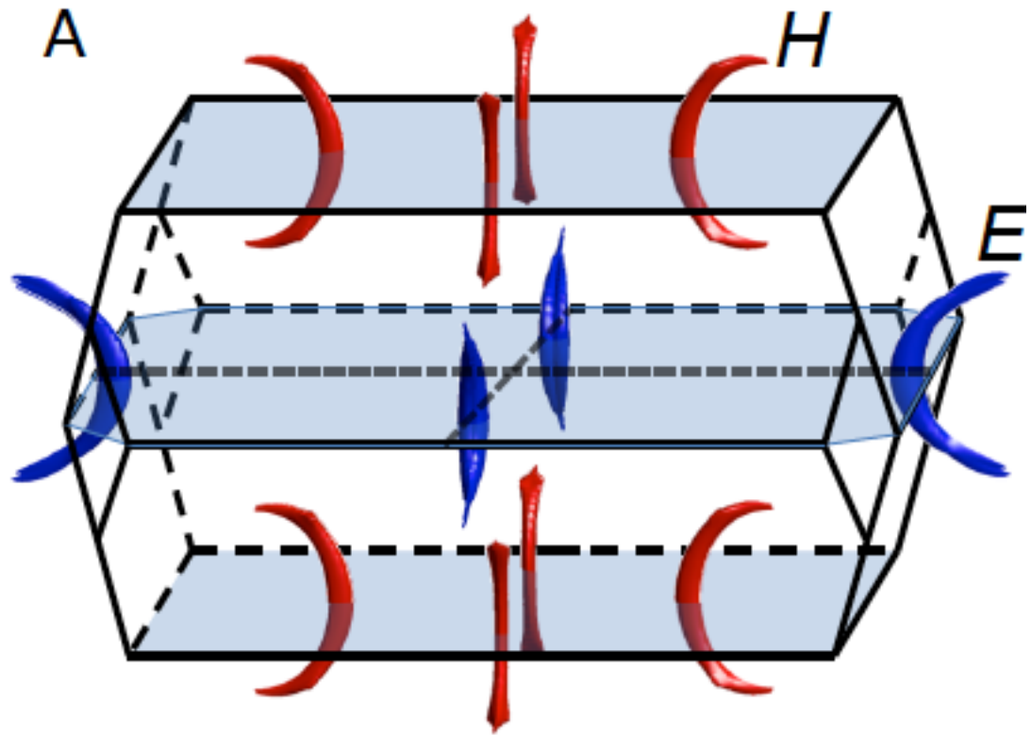

Along nodal rings
FS pockets contain pairs of Weyl points

Position of Fermi level with respect to Weyl points

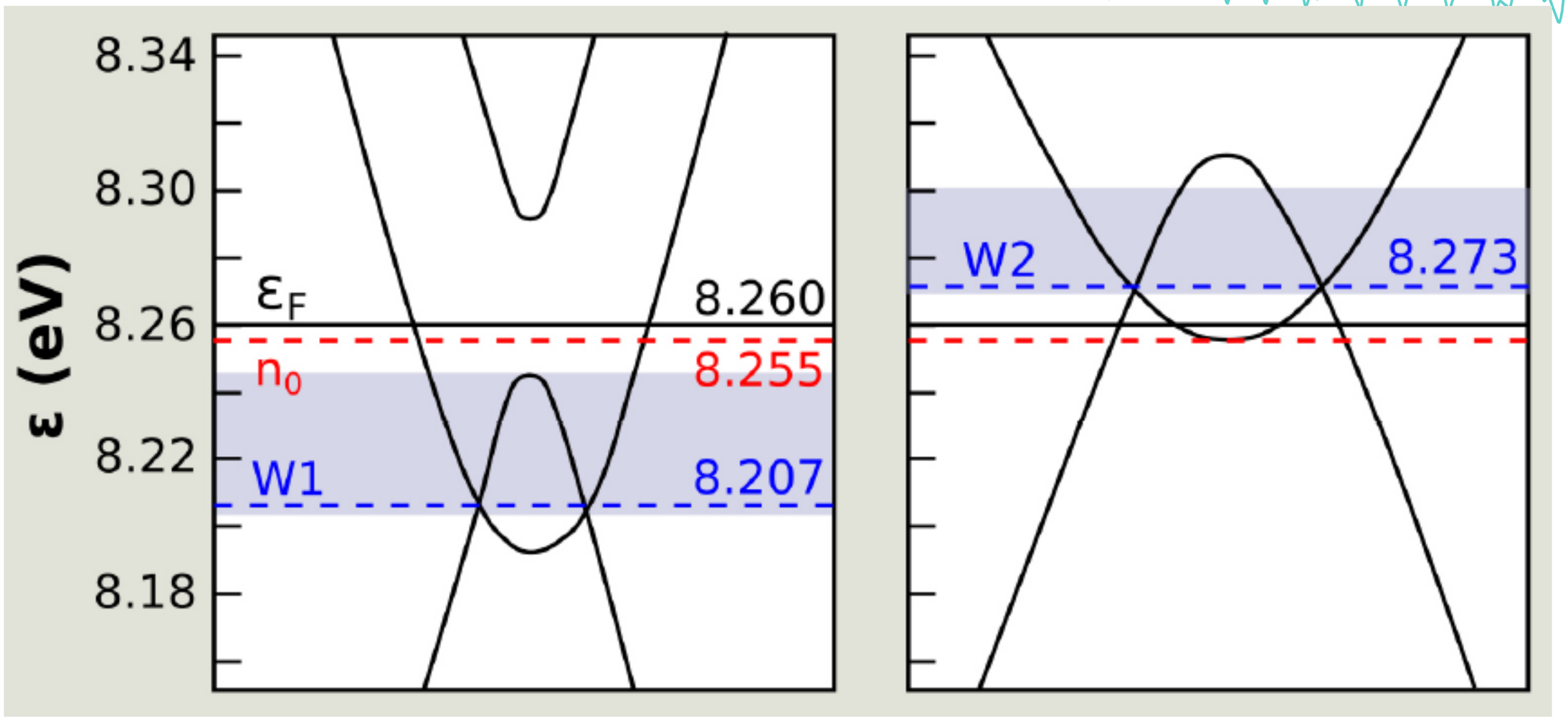

Determined Fermi level with meV resolution

E_F is 5 meV above charge neutral Fermi level

In agreement with Hall measurements

Carrier density: n ≈10^{19}

TaP

- No independent Fermi surface pockets around Weyl points

- No well-defined chirality

- Physical properties based on chirality such as chiral anomaly not expected

Negative longitudinal magnetoresistance

TaP

I || a B || a

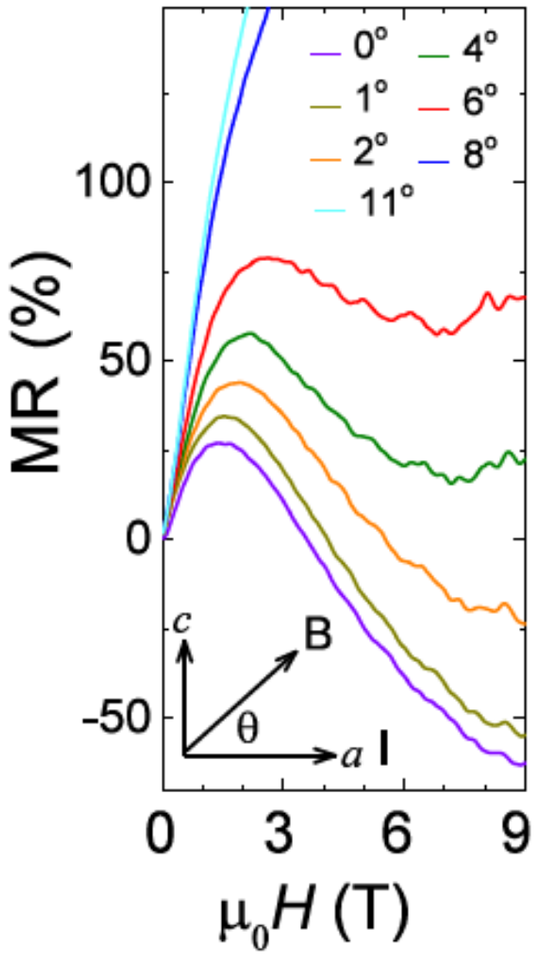

I || c B || c

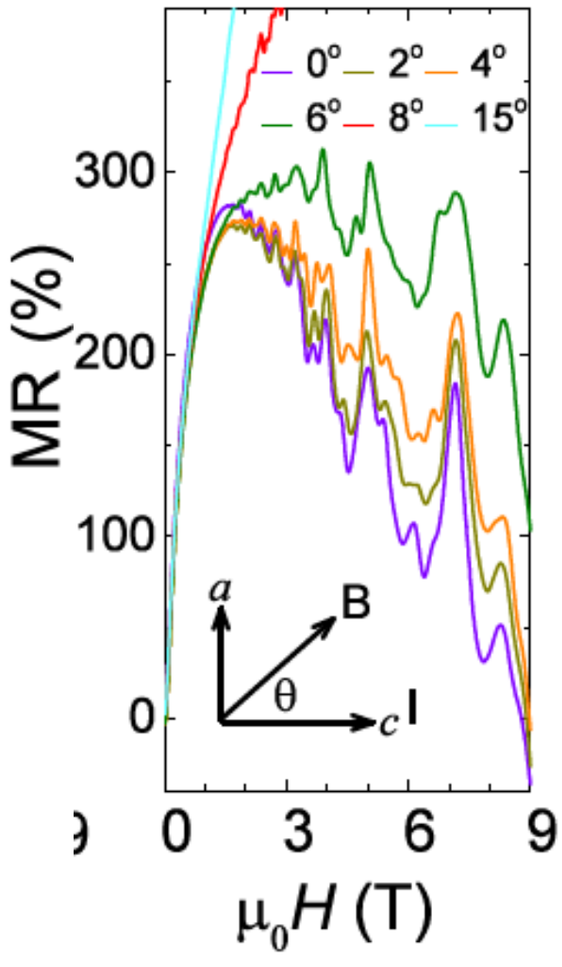

Appears in very small angular window

I and B have to be parallel within 2°

Inhomogeneous current distribution

Point-like contacts

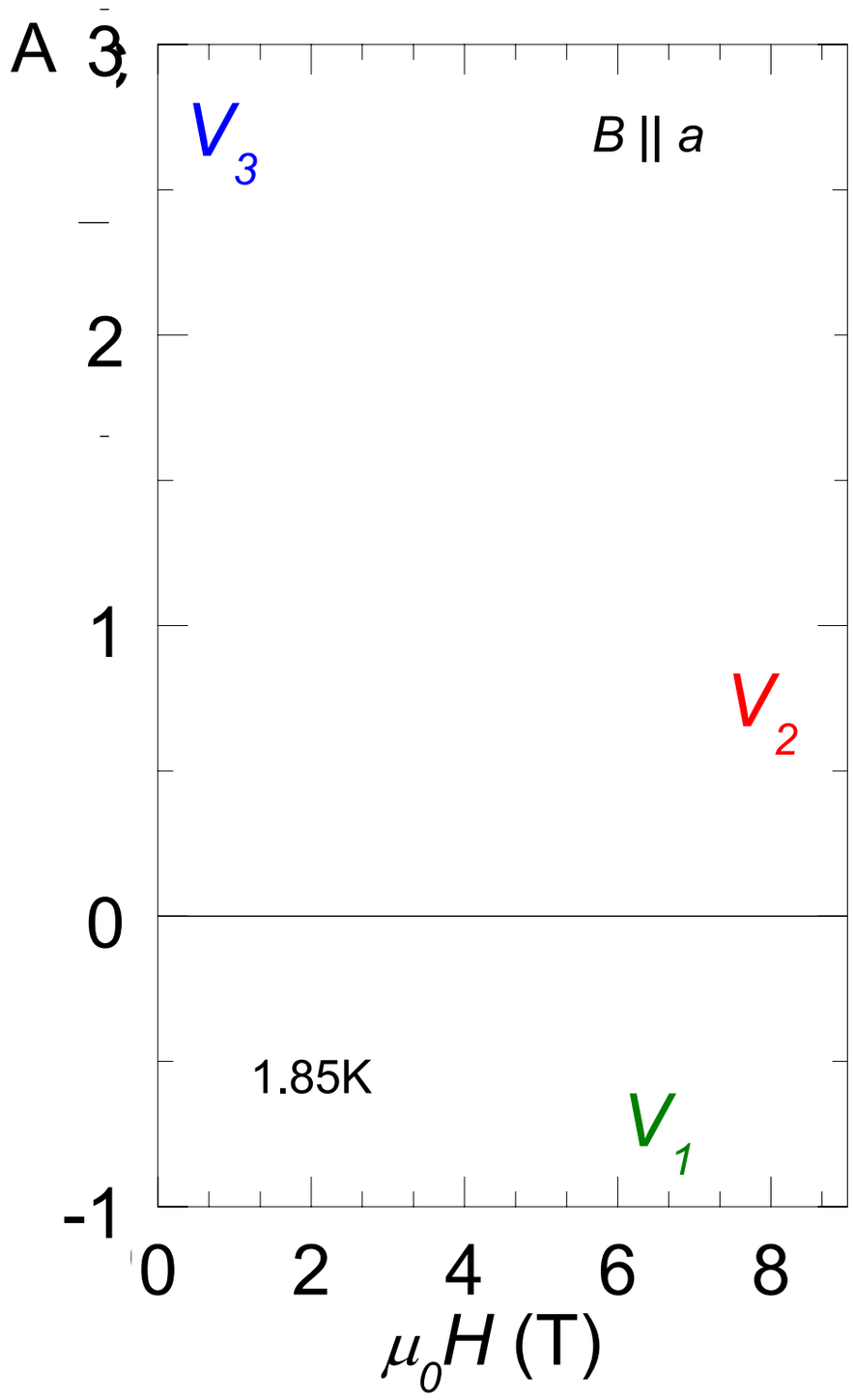

Reed 1971
Yoshida JPSJ 1975
Pippard, Magnetoresistance in Metals

Large transverse magnetoresistance

I || a B || c

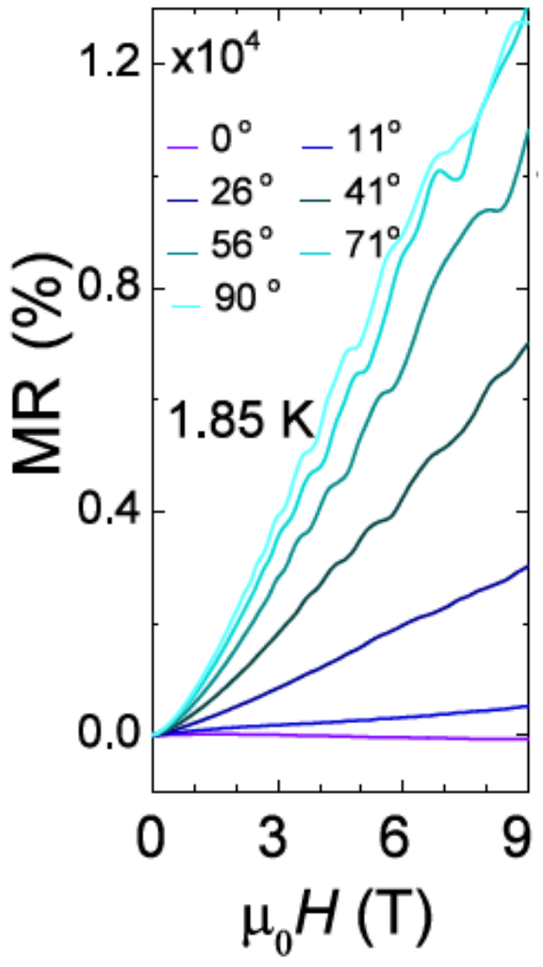

I || c B || a

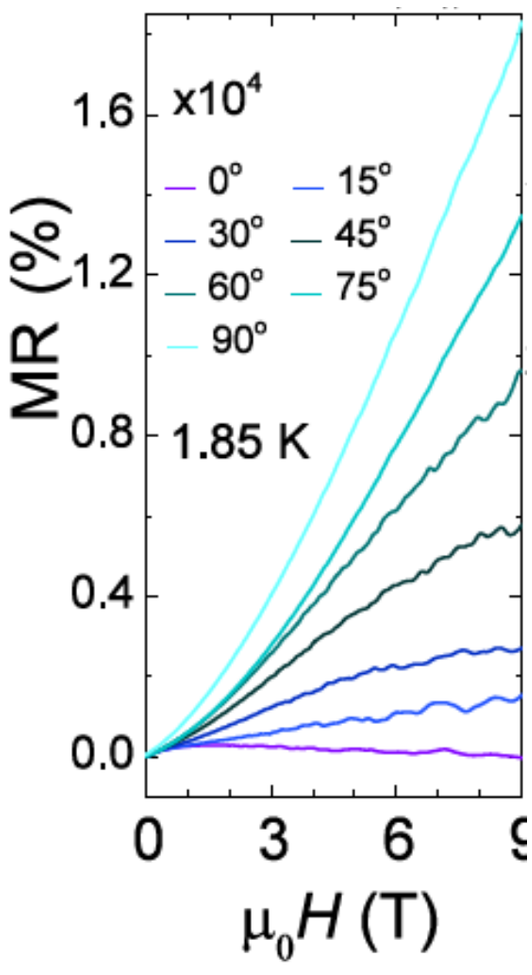

- Large transverse MR due to strong orbital effect
- Orbital effect absent in longitudinal magnetic fields

High mobility: $\mu B = \omega_c \tau$

Anisotropy over $R_t / R_l > 100$

Potential distribution in systems with anisotropic resistivity tensor

$H = 0$ $H > 0$

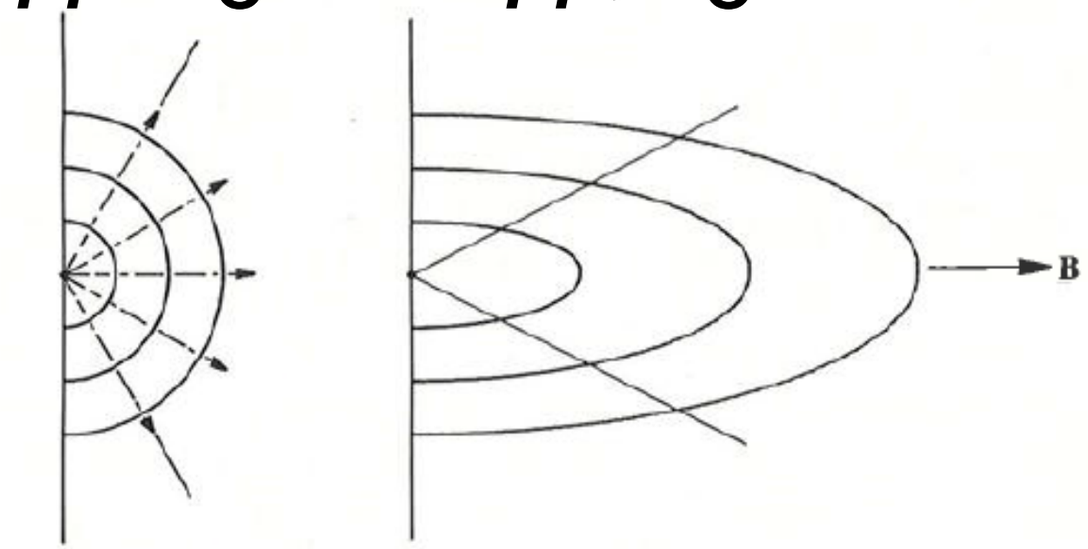

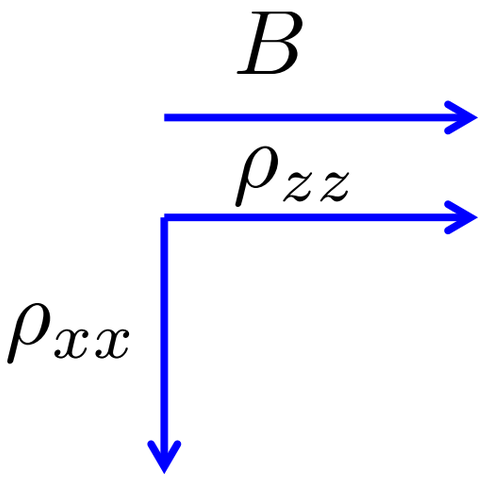

$$A = \frac{\rho_{xx}}{\rho_{zz}}$$

Yoshida JAP 1980
Pippard, Magnetoresistance in Metals

Current trajectory

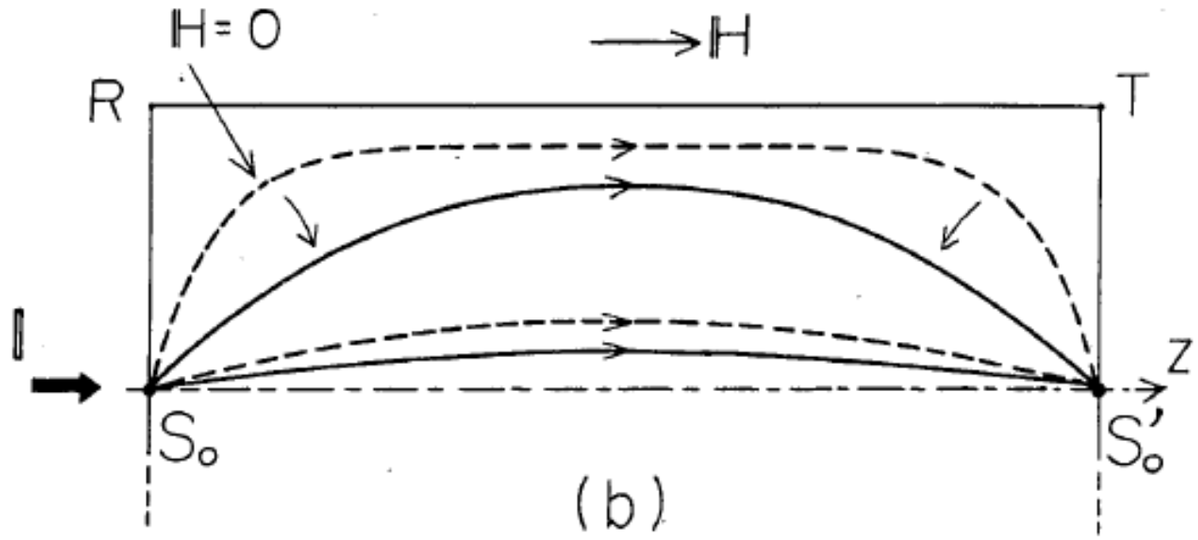

Potential distribution

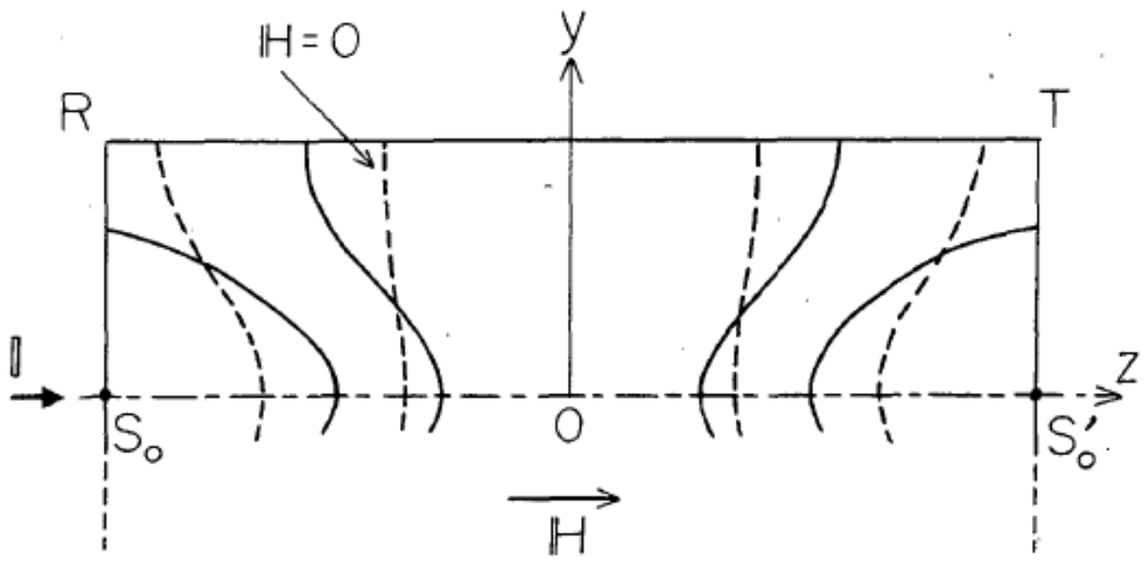

Inhomogeneous current distribution

Point-like contacts

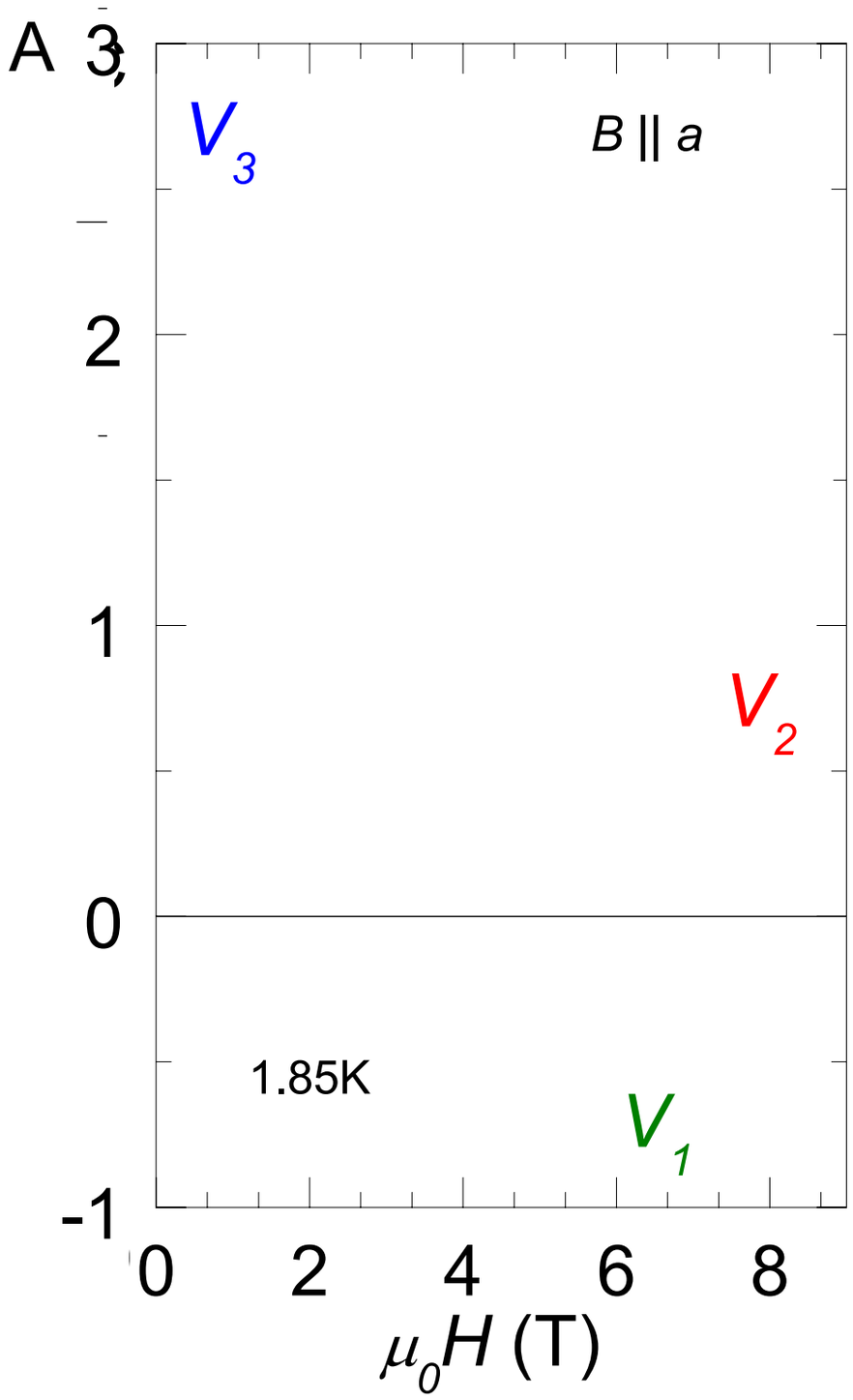

Bismuth 1976

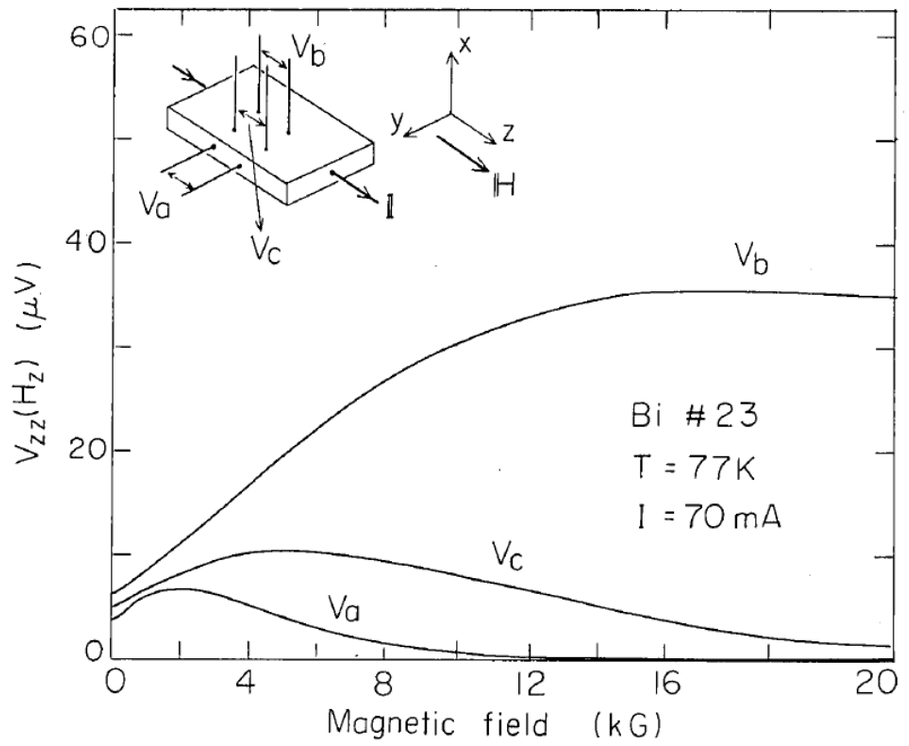

Reed 1971
Yoshida JPSJ 1975
Pippard, Magnetoresistance in Metals

Current jetting

Equipotential lines

$B \longrightarrow$

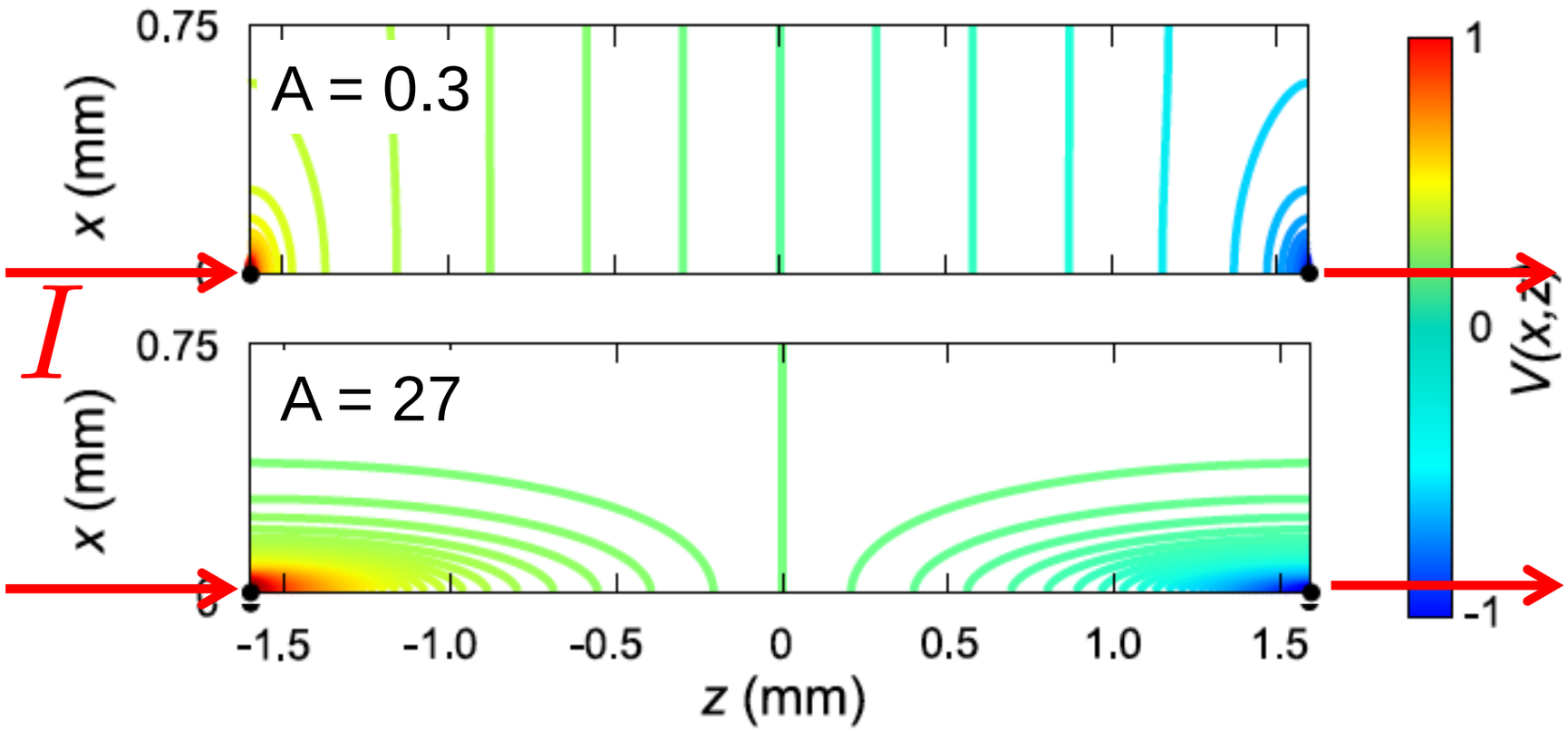

Resistance anisotropy $A = R_t / R_l = 27$

Yoshida JAP 1980
Pippard, Magnetoresistance in Metals

Inhomogeneous current

Point-like contacts
$R_I = R_I(0\ T)$

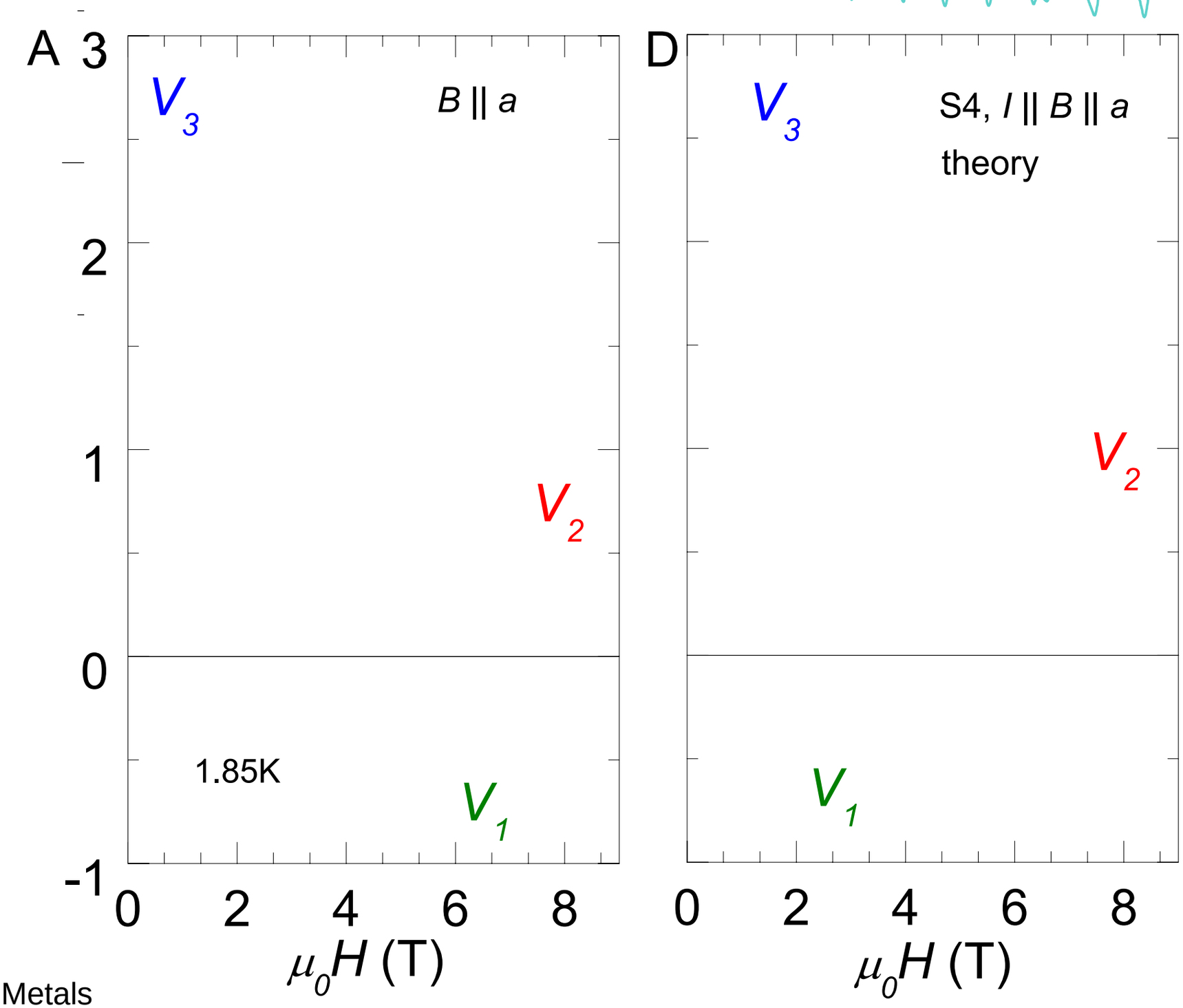

Reed 1971
Yoshida JPSJ 1975
Pippard, Magnetoresistance in Metals

The case of NbP

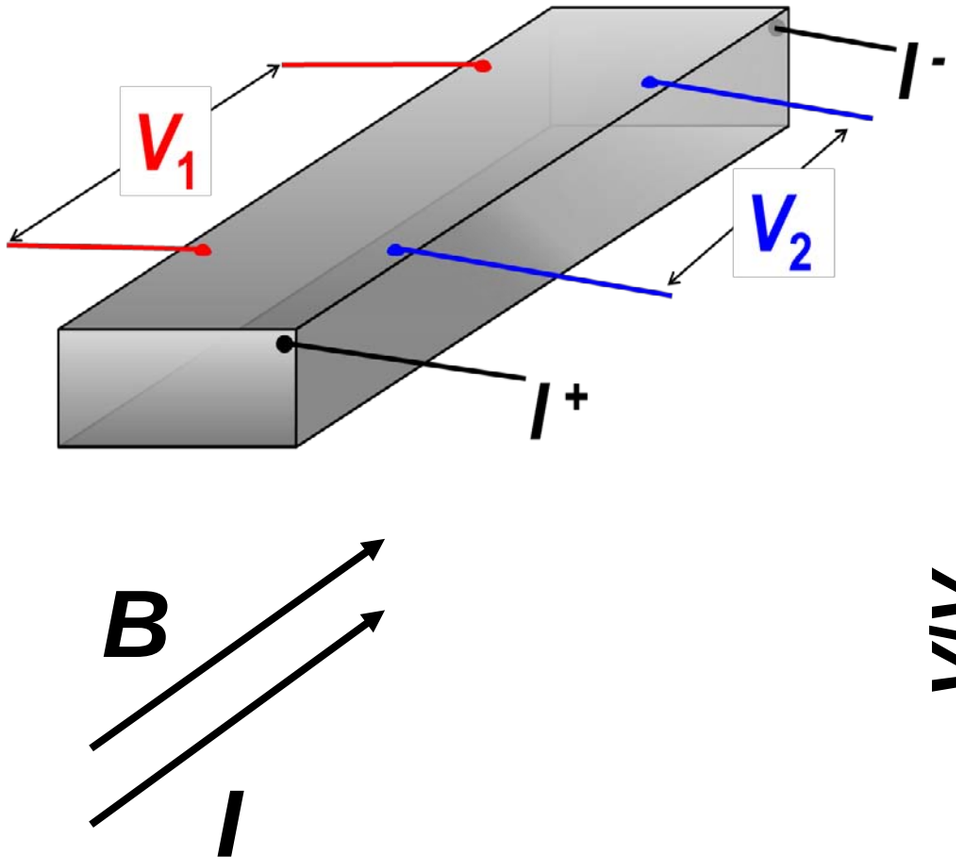

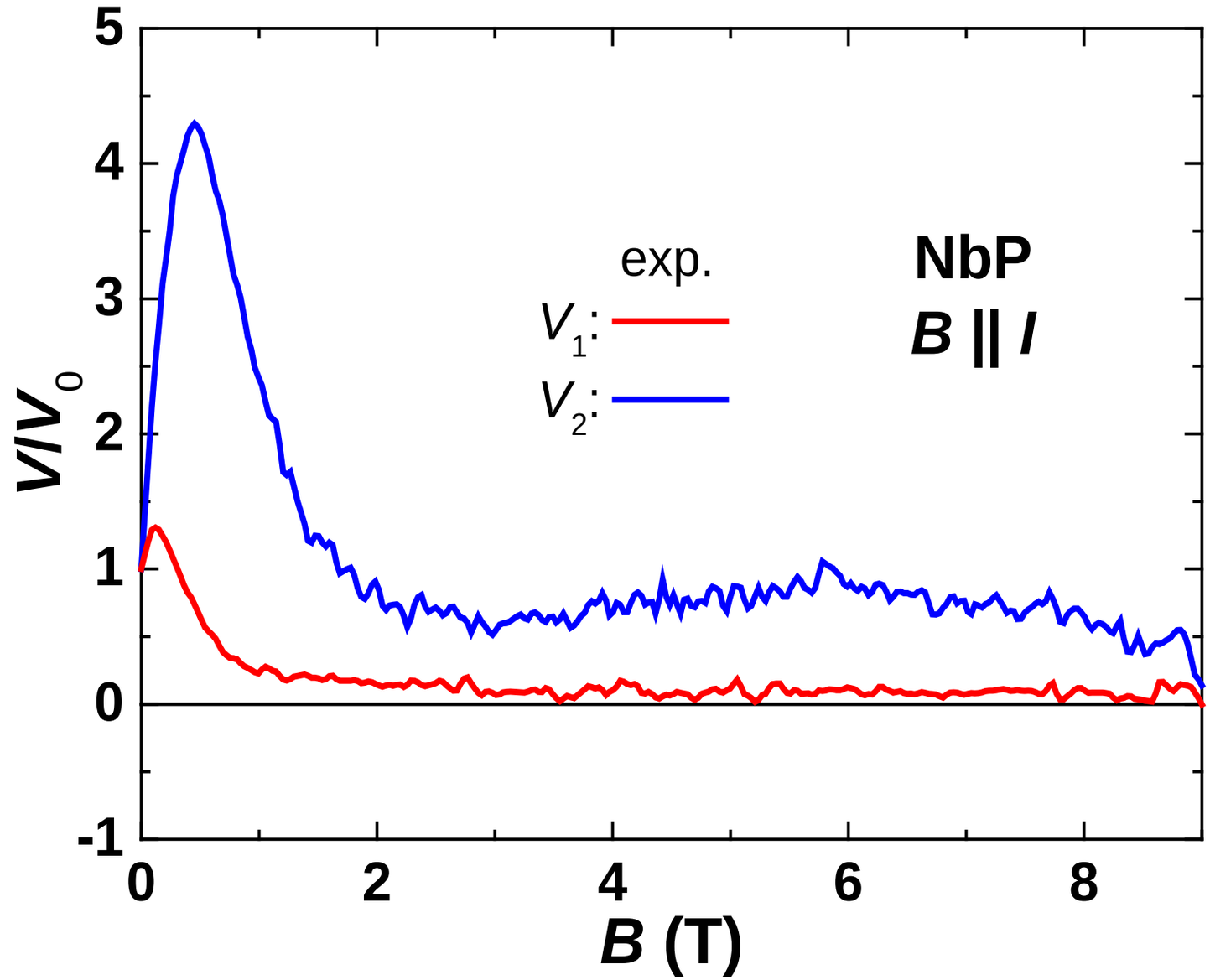

Finite element simulations

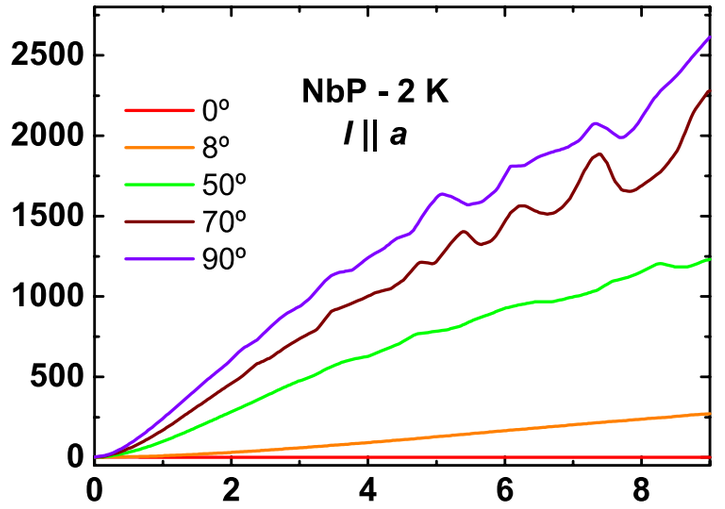

ρ_{xx} is obtained from the transversal MR ($B \perp I$)

ρ_{zz} is assumed field independent- $\rho_{zz}(B) = \rho_{zz}(B=0)$

$A = \rho_{xx}(B) / \rho_{zz}(B) = \rho_{xx}(B) / \rho(0)$

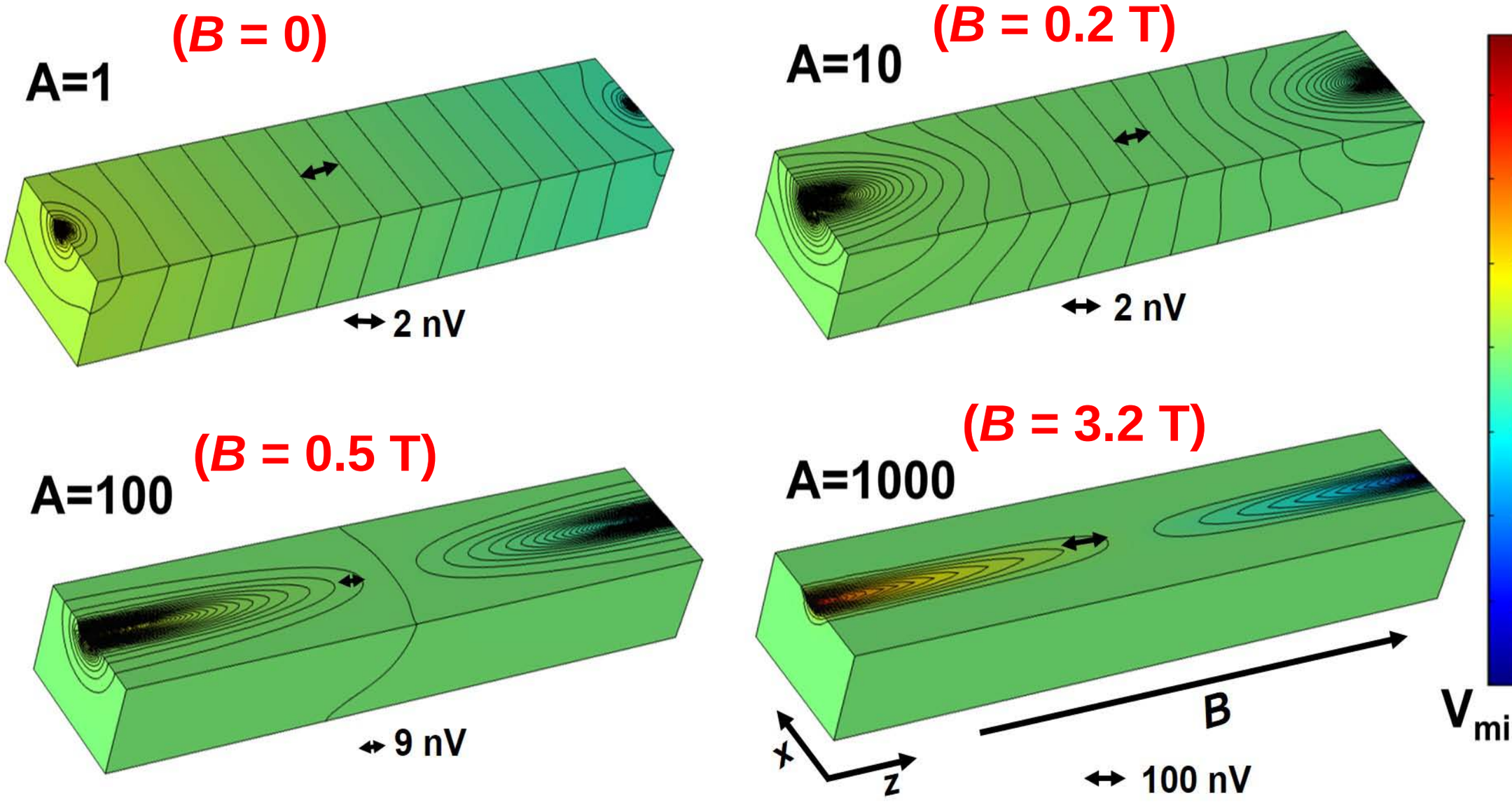

Comparison with experiment

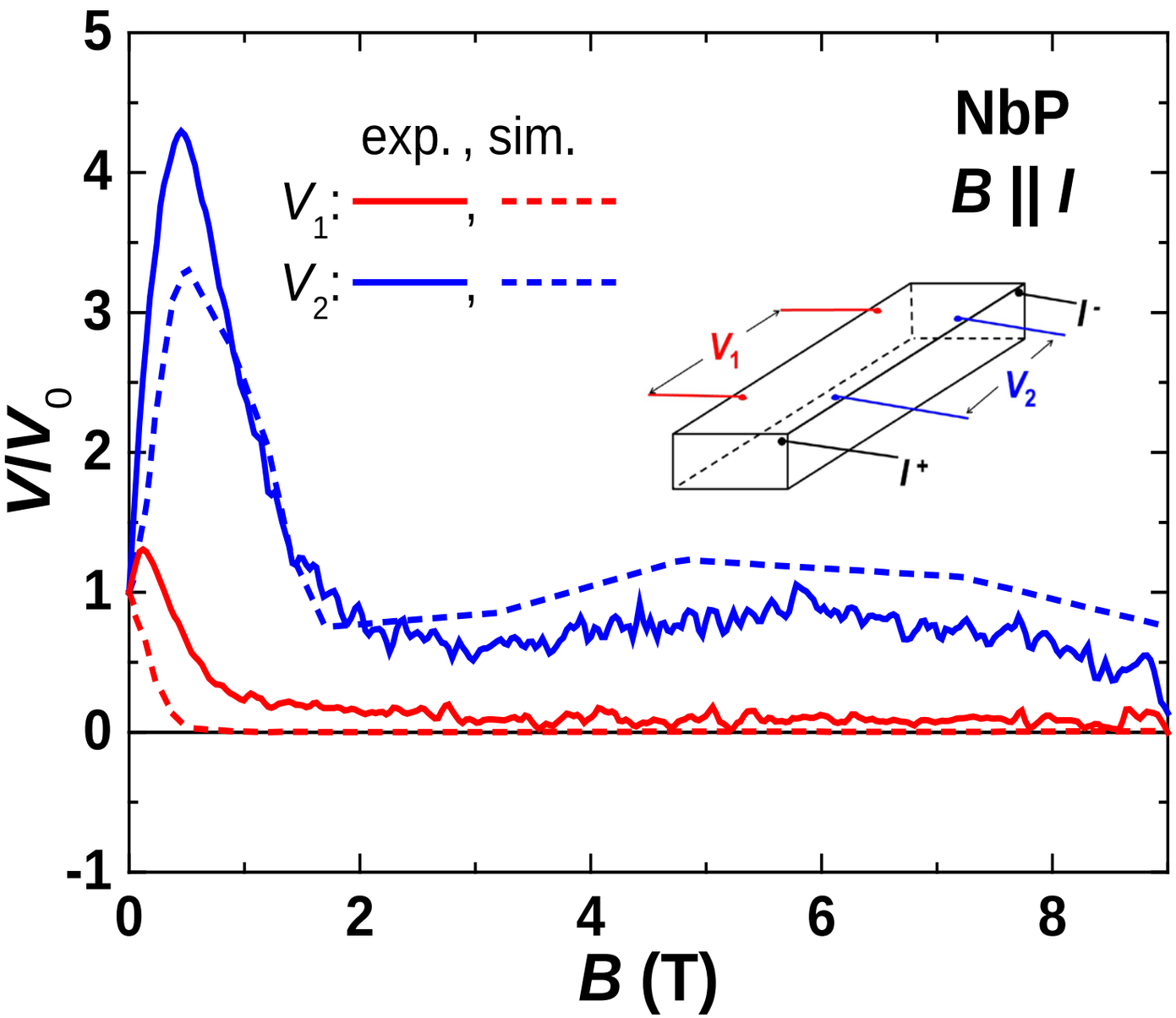

- The voltage drop is caused by increase of the transverse MR (anisotropy *A*)
  → the current concentrates along a straight line connecting the current electrodes.

- The increase of V_2 below 1 T occurs because the effective cross section of the sample is reduced → higher currents and voltages close to the current jet.

Angular dependence

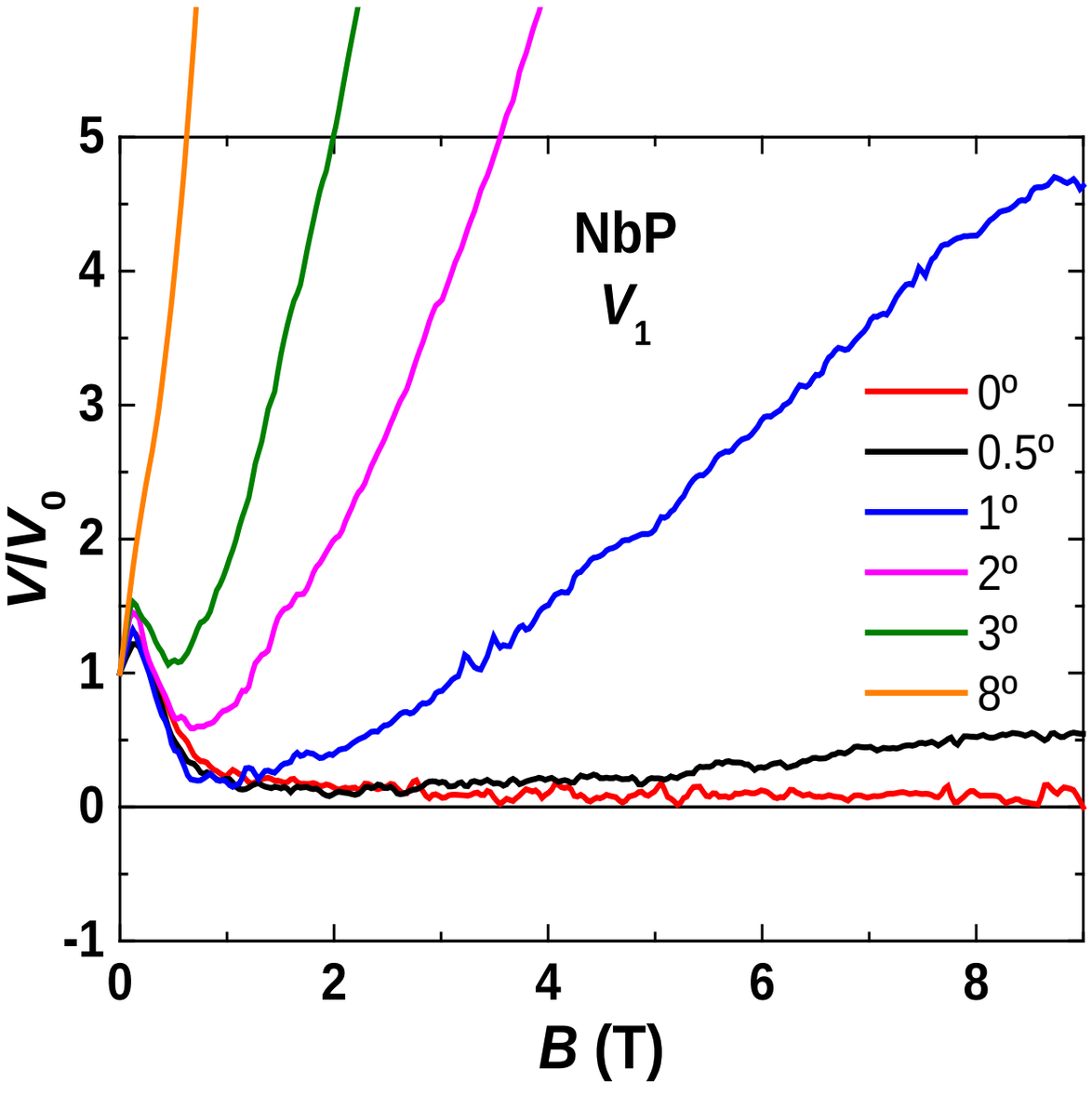

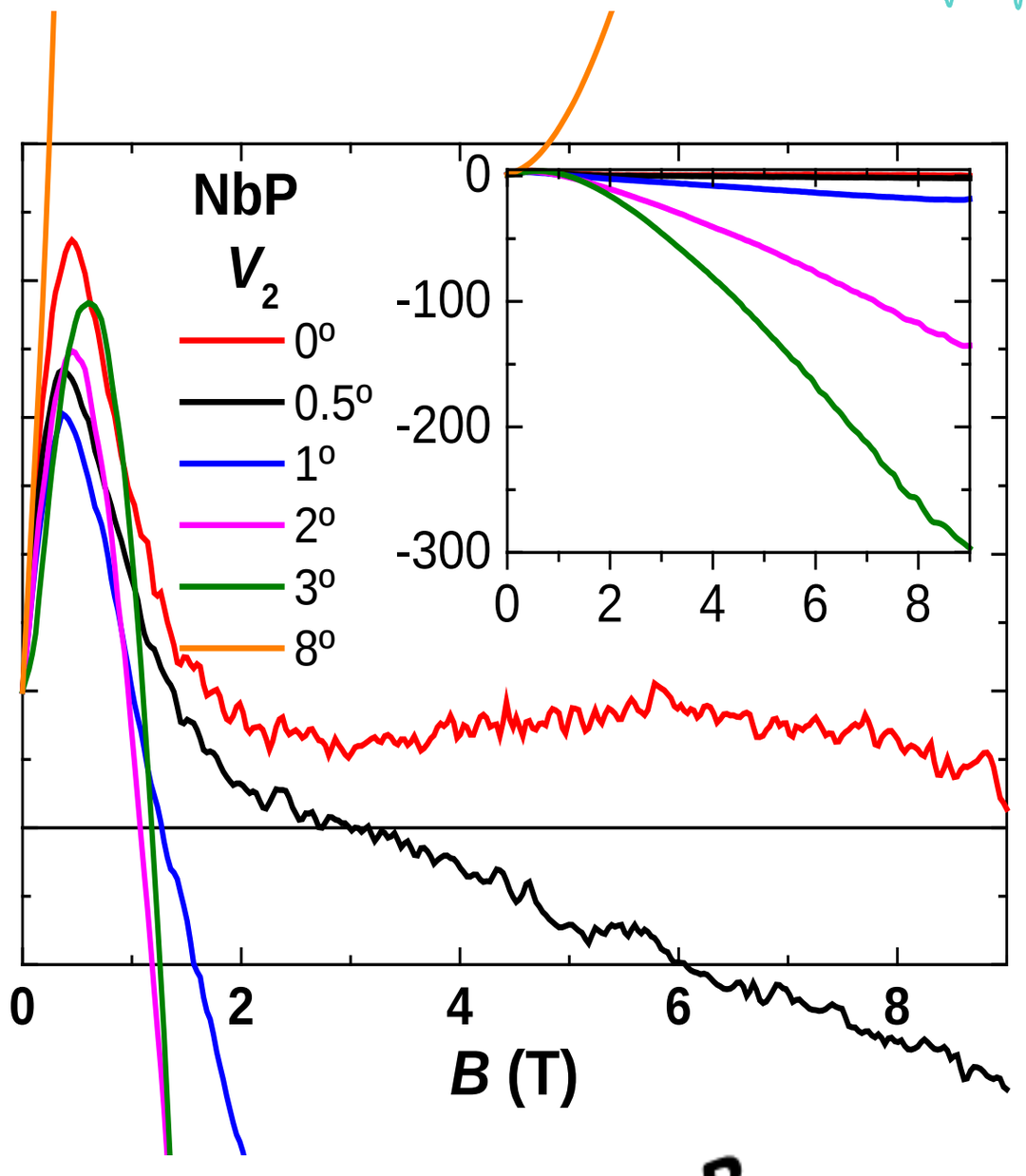

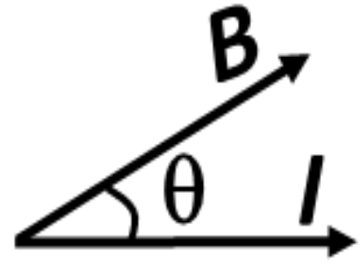

Inhomogeneous current

A similar angular dependence has been reported for Sb about 40 years ago.

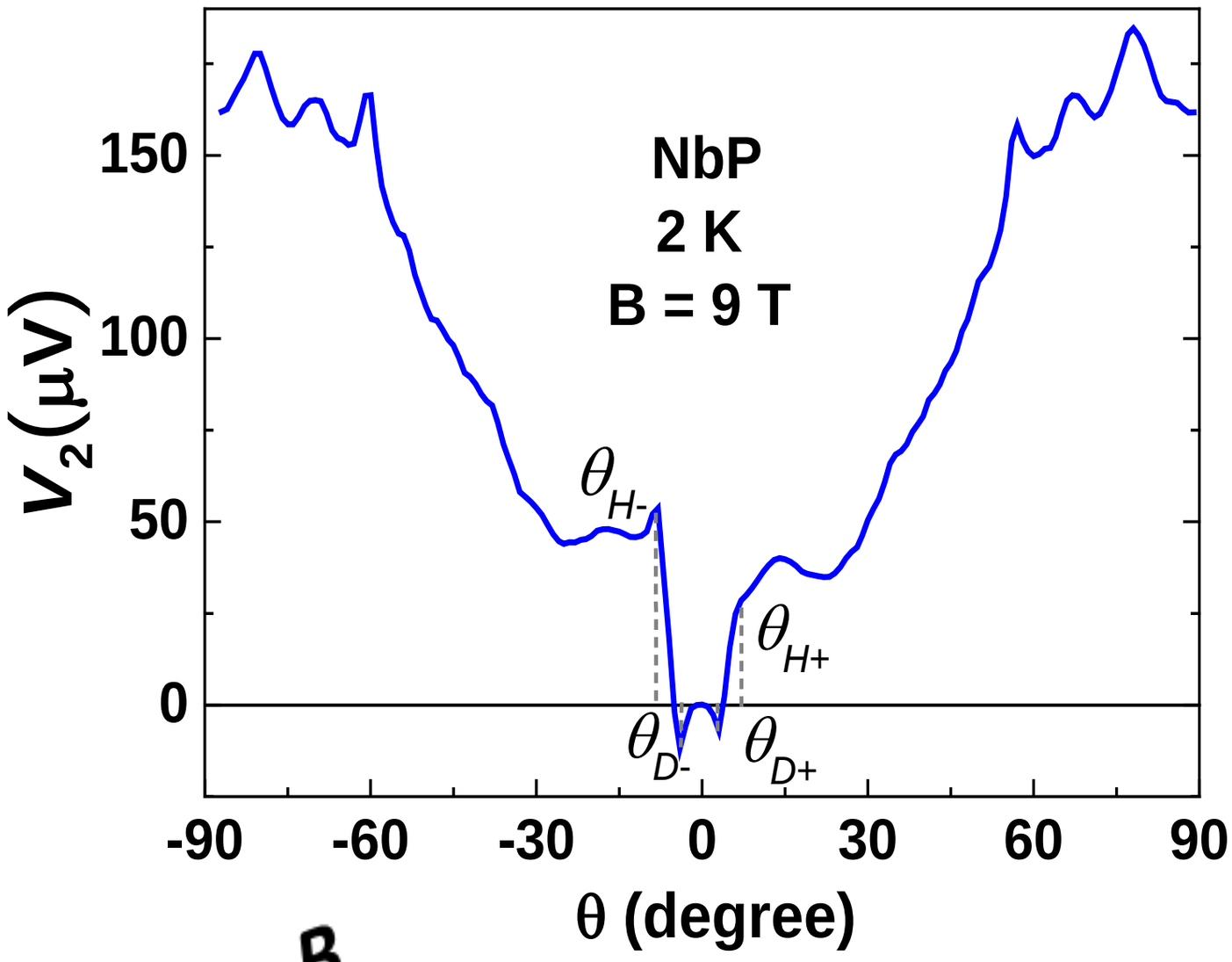

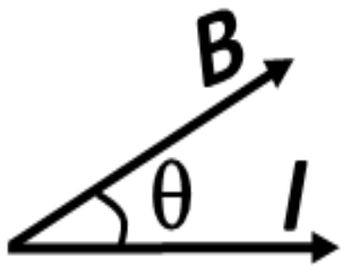

Yoshida JPSJ 1975

Potential distribution for tilted magnetic field

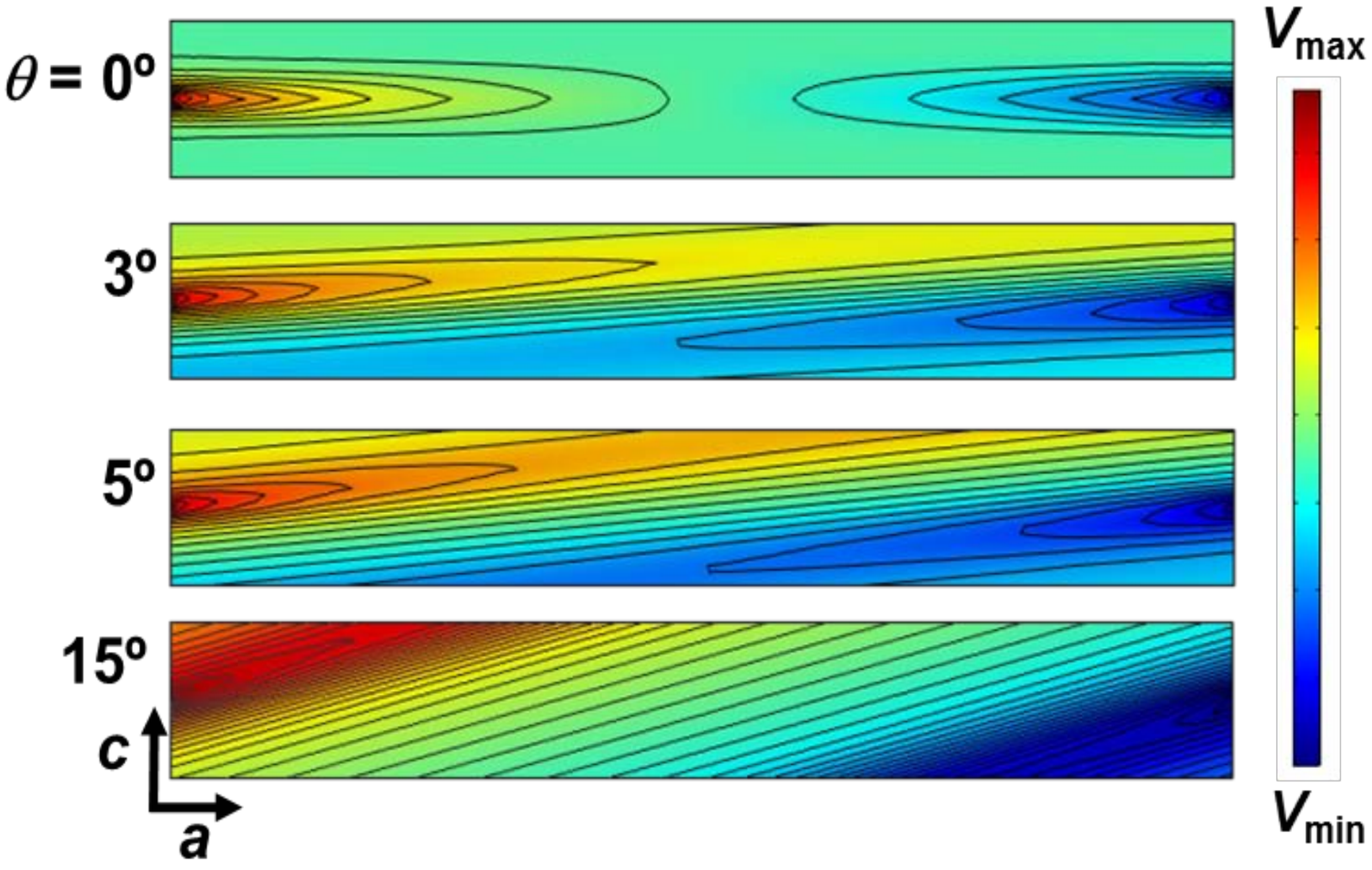

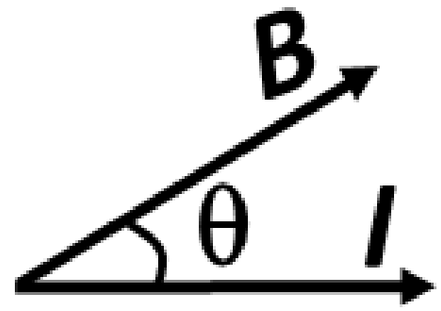

Current rotates with the magnetic field

Geometric determination of dip and hump angles

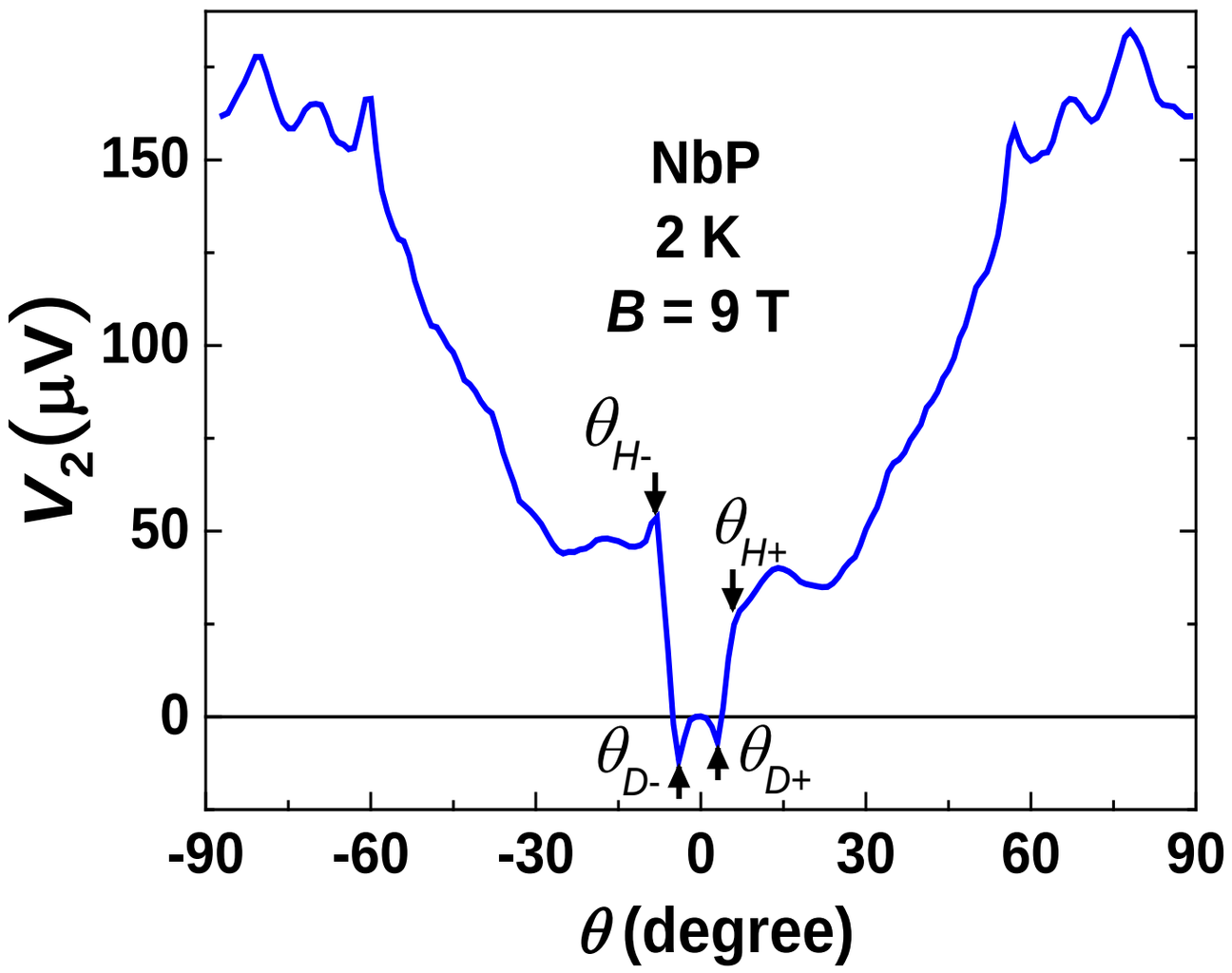

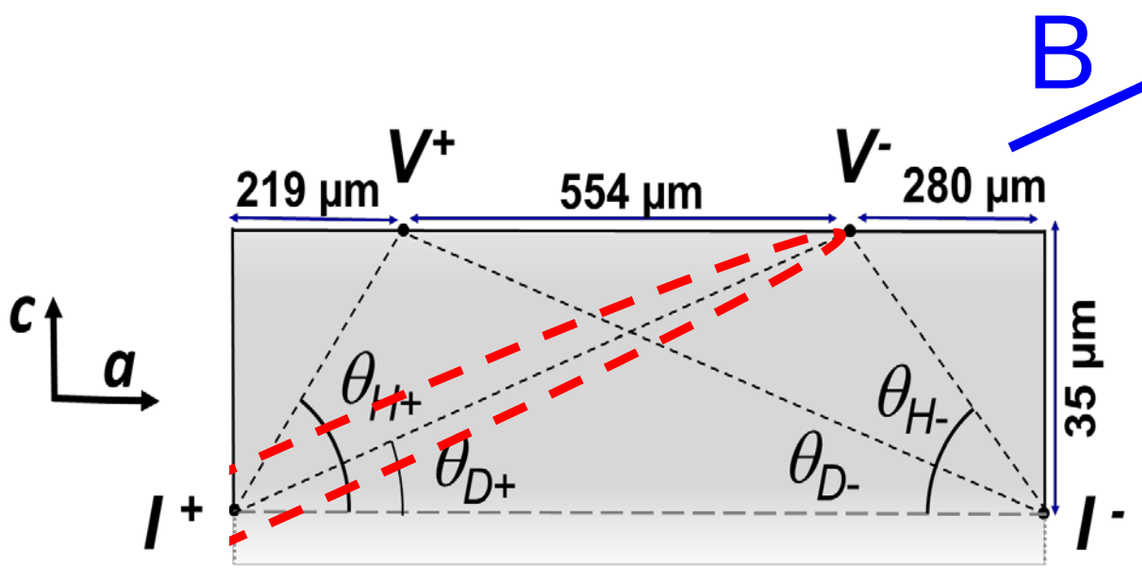

Good agreement between the angles observed in the experiment and the angles expected from the geometry.

Chiral anomaly?

- Current jetting is a general phenomenon appearing in longitudinal MR measurements when the resistance anisotropy changes in field, even for low anisotropies (low fields or high temperature)
- Explains naturally the field dependence of the measured signal (small hump for low fields, reduction of voltage)
- Explains naturally the angle dependence ($\neq \mathbf{E} \bullet \mathbf{B}$)
- Measurements of longitudinal MR have to be carefully checked in order to exclude the current jetting
- Effect of chiral anomaly might exist but we need better measurements

TaAs – Quantum oscillations

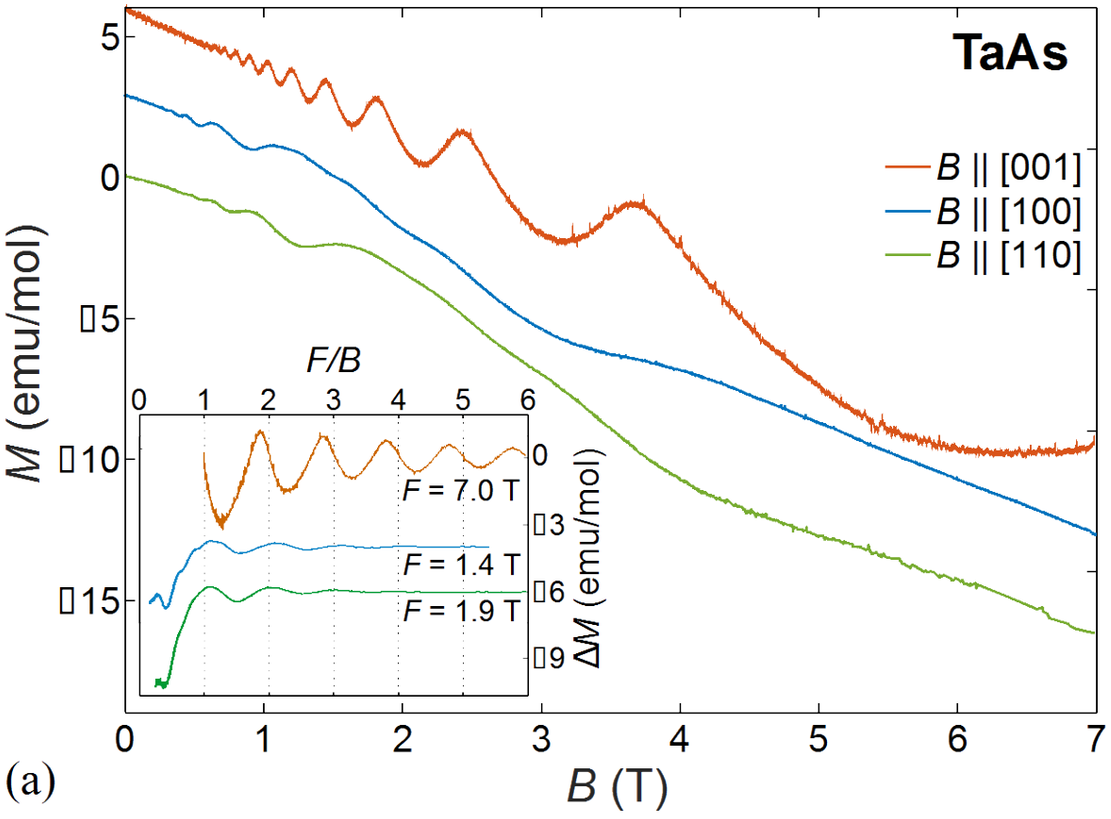

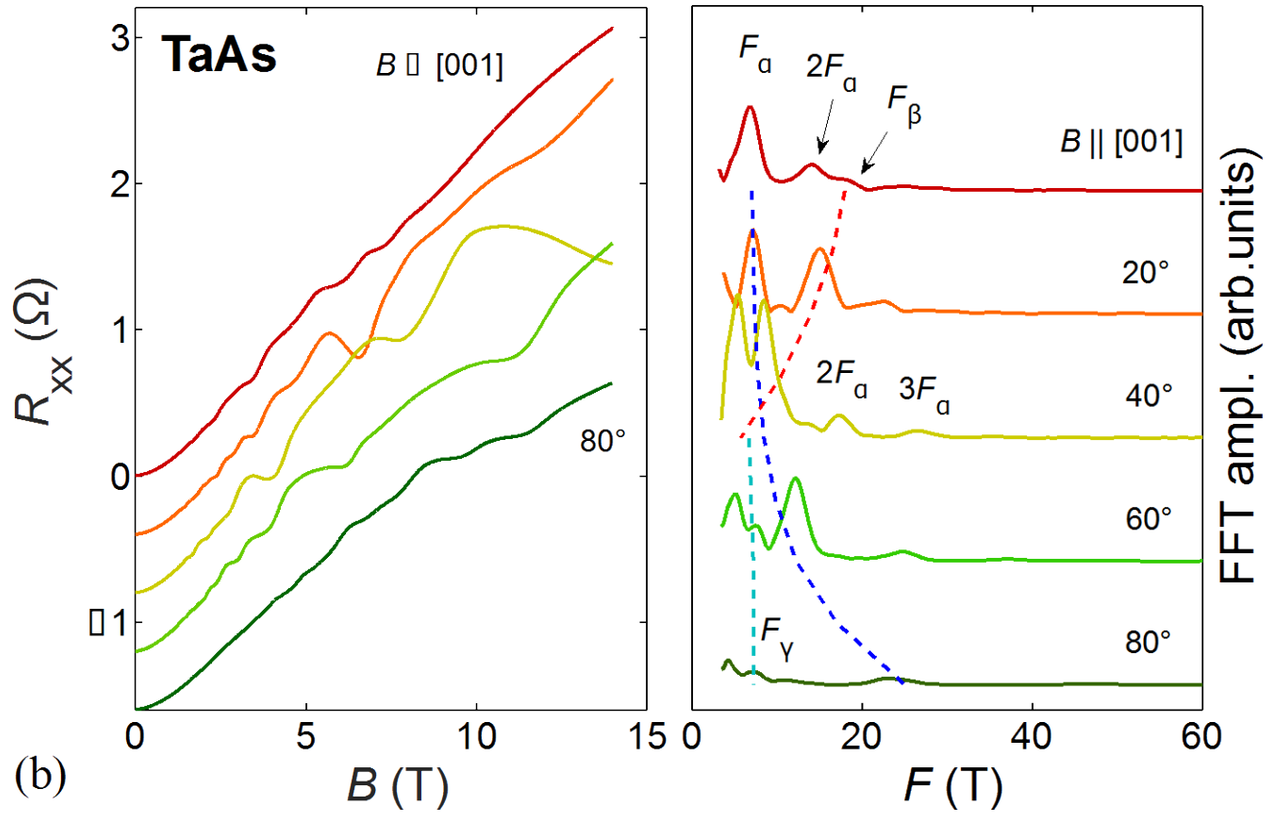

- Diamagnetic, strong QO in all directions
- Two new oscillation frequencies compared to other studies

Angular dependence

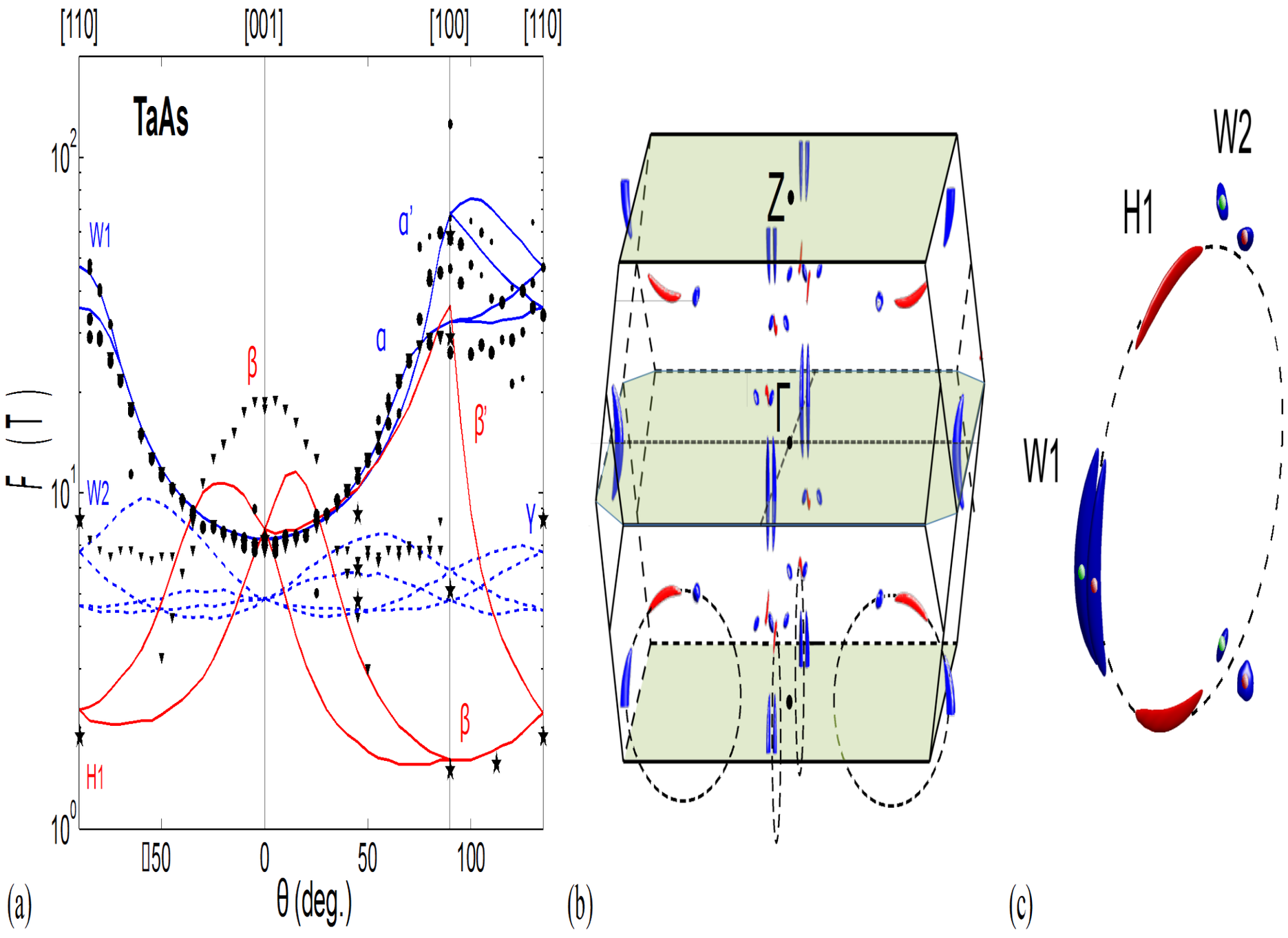

How do we determine the Fermi energy?

TaAs – oscillation frequency as a function of the Fermi energy

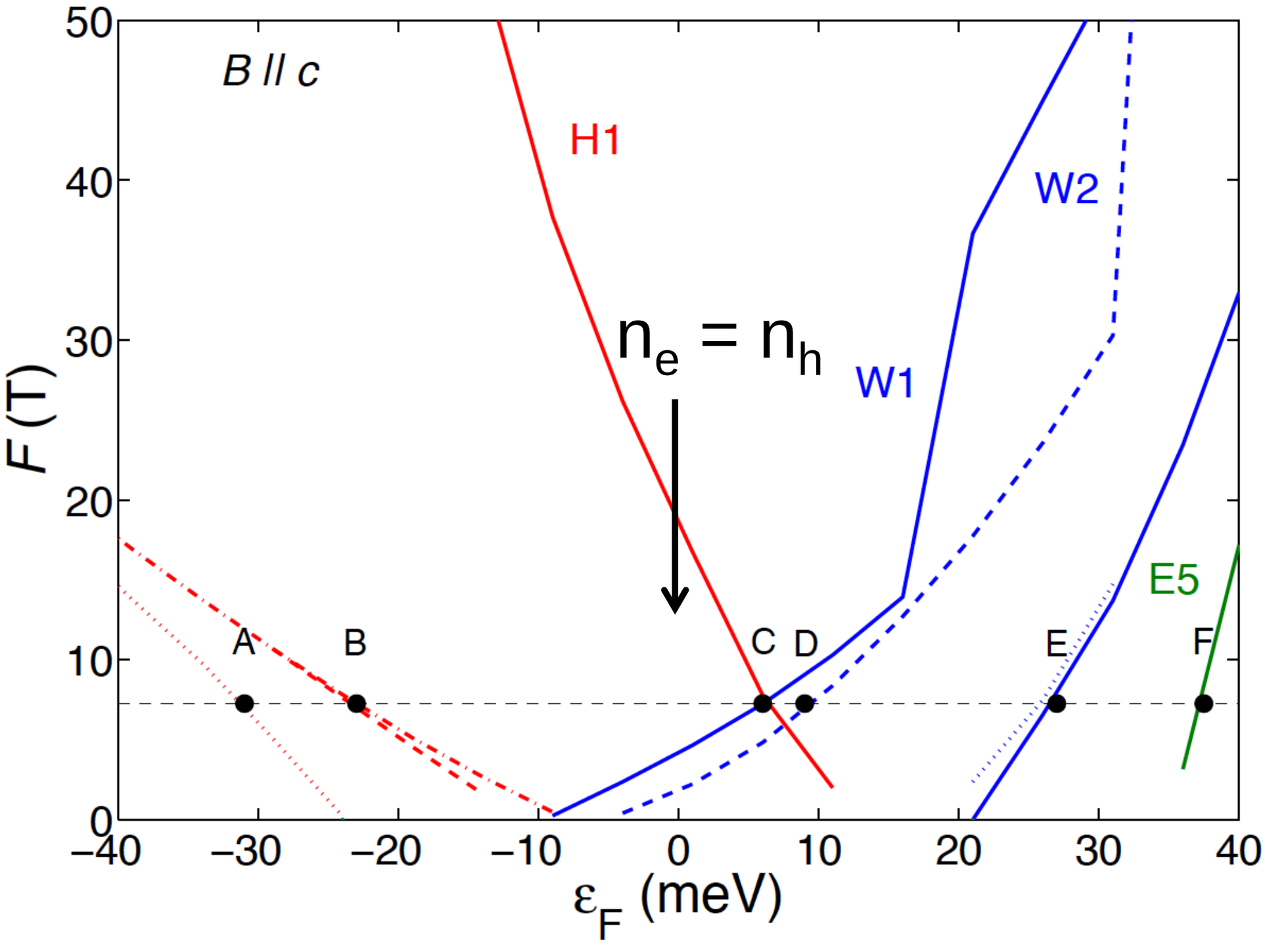

TaAs

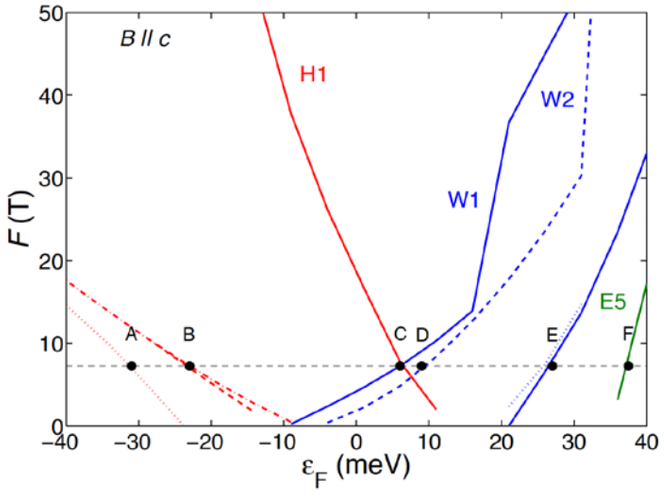

A
$-32\,\mathrm{meV}$

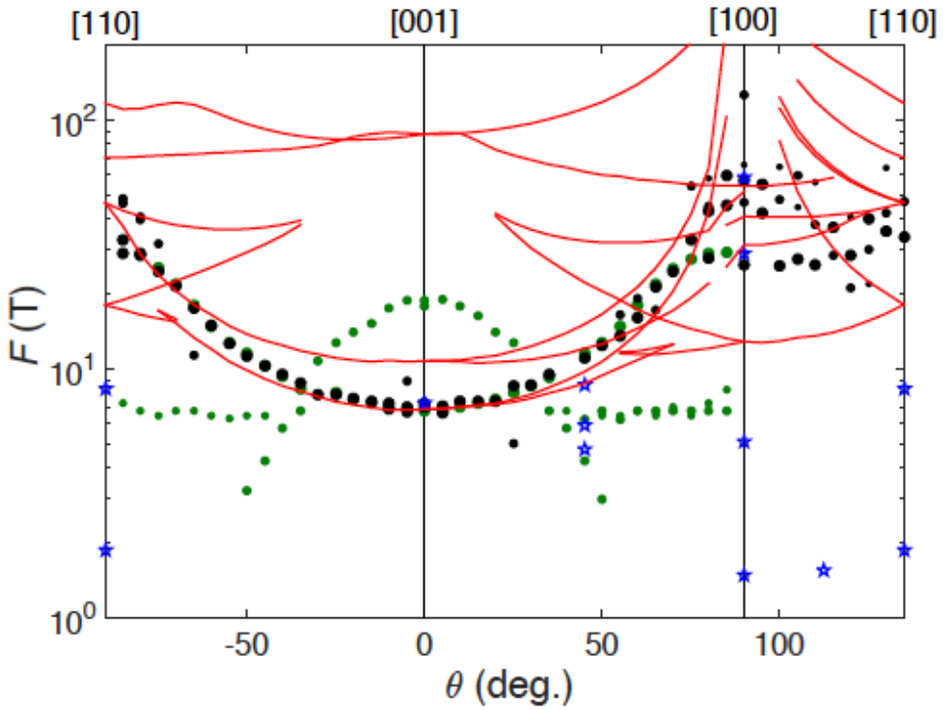

B
$-23\,\mathrm{meV}$

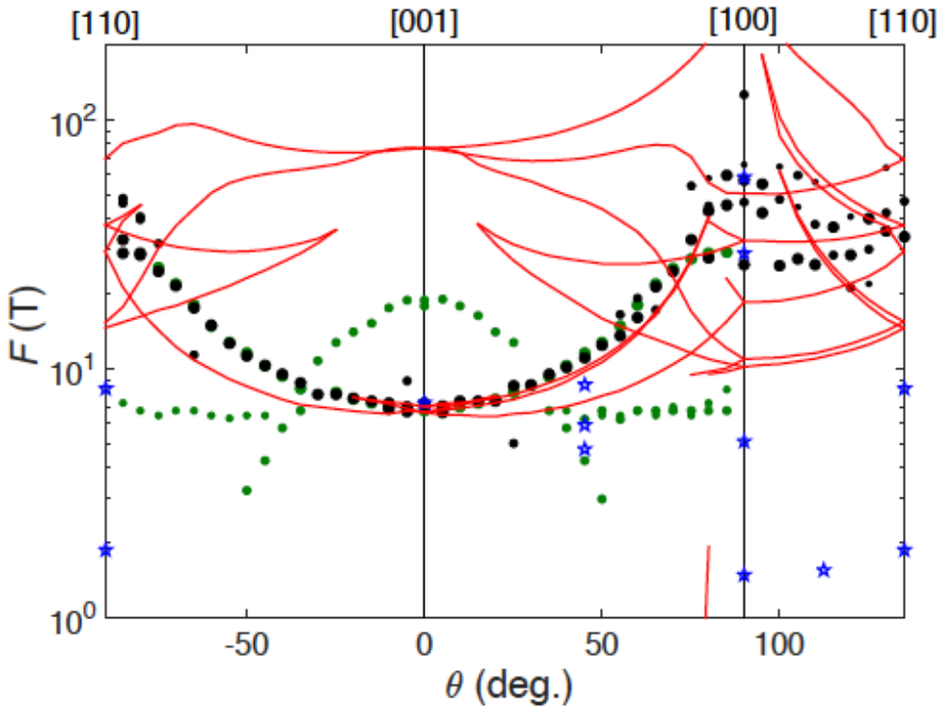

TaAs

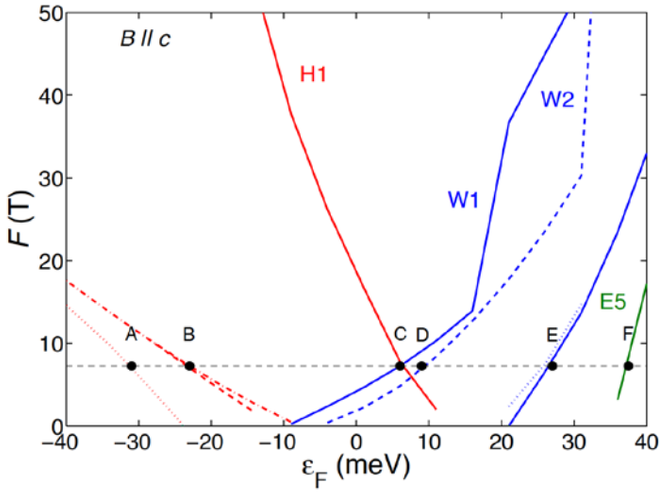

C
+6 meV

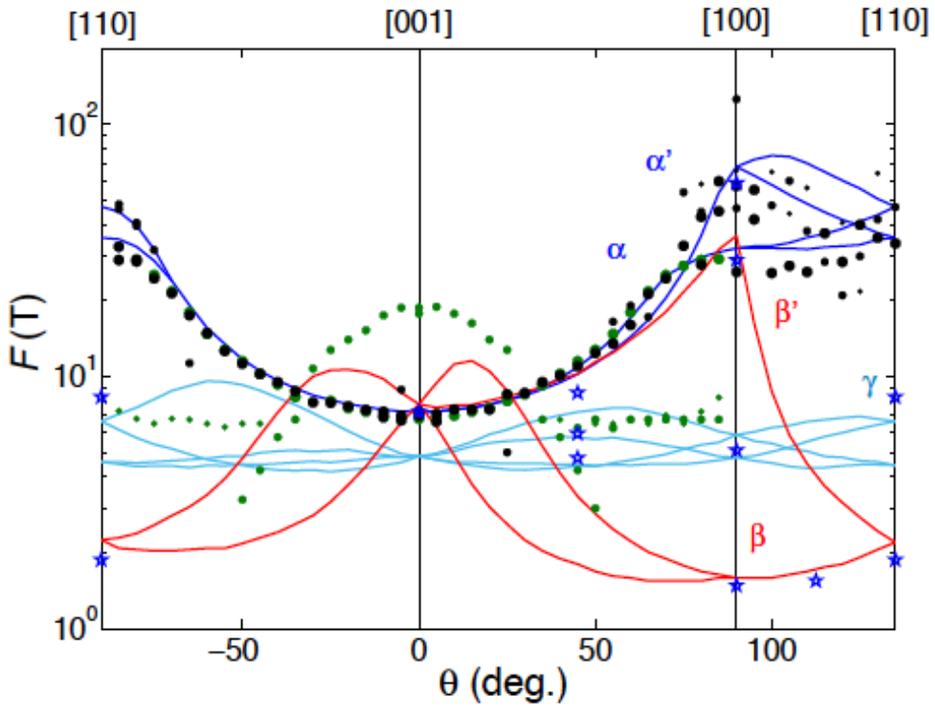

D
+9 meV

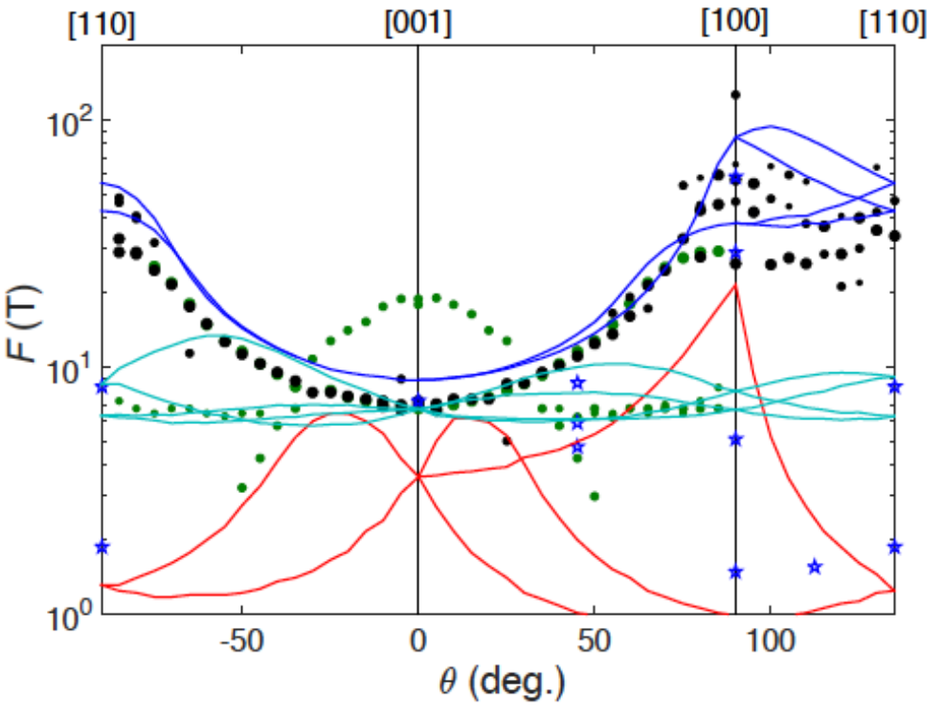

TaAs

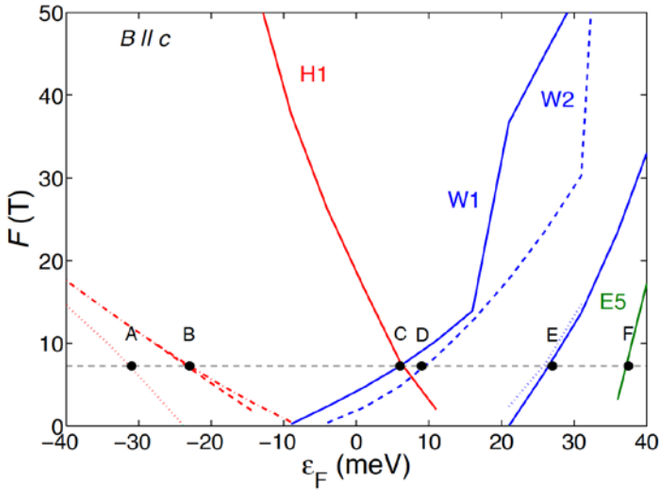
B // c
H1
W2
W1
E5
A
B
C D
E
F
F (T)
ε_F (meV)

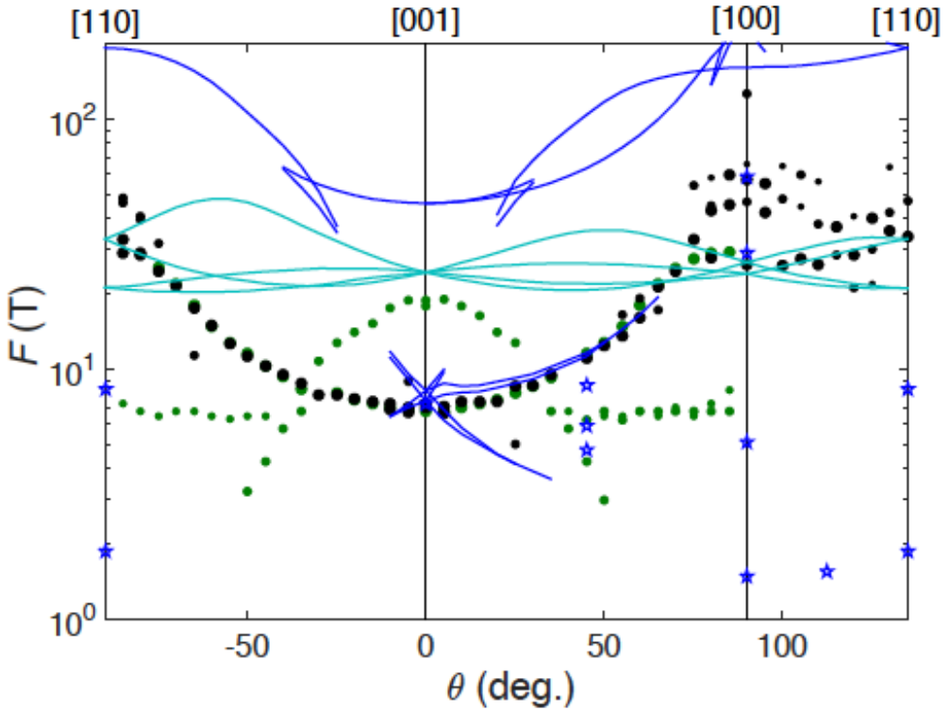
[110]
[001]
[100]
[110]
F (T)
θ (deg.)

E
+27 meV

TaAs - Fermi surface

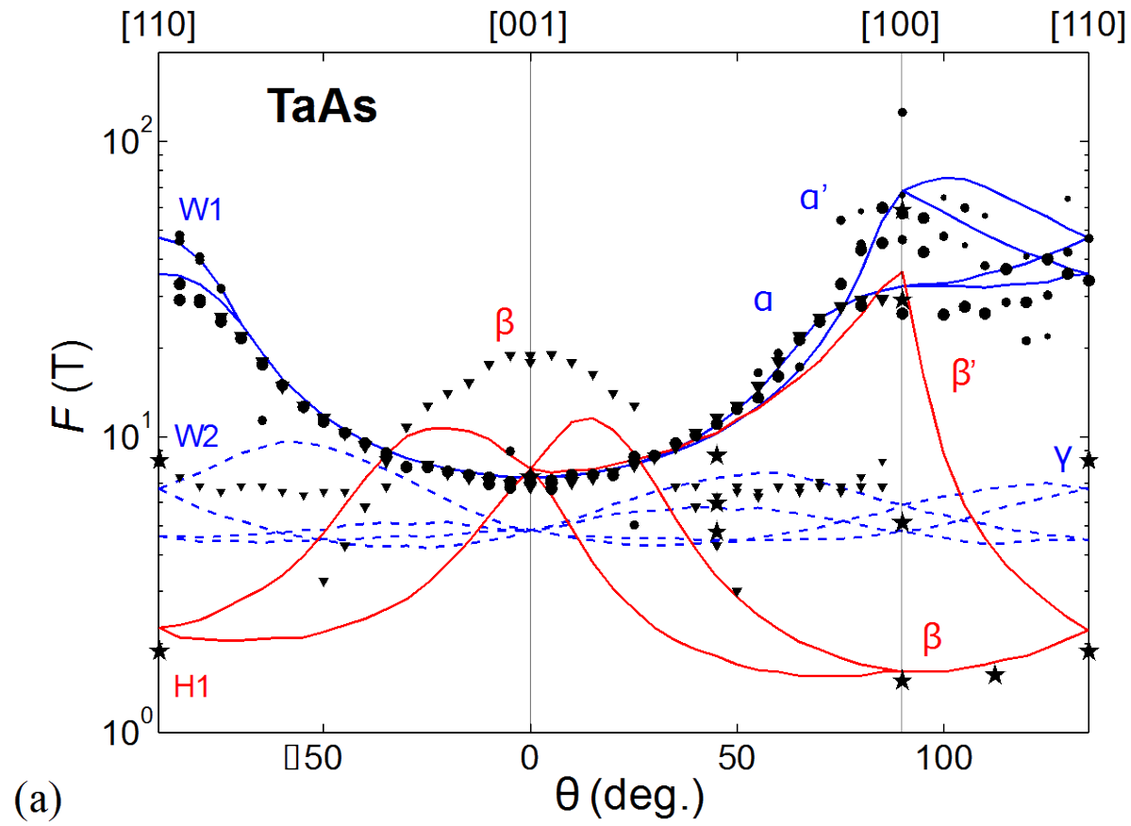

(a)

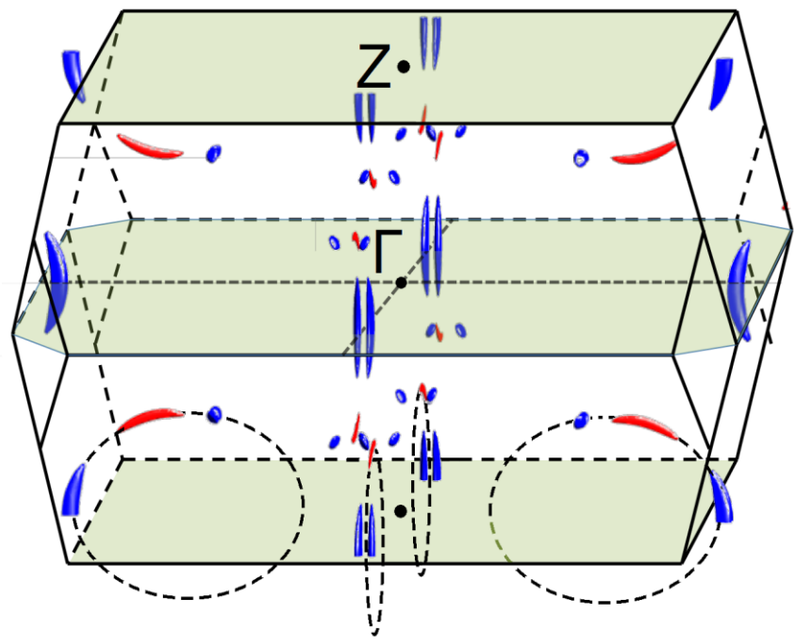

(b)

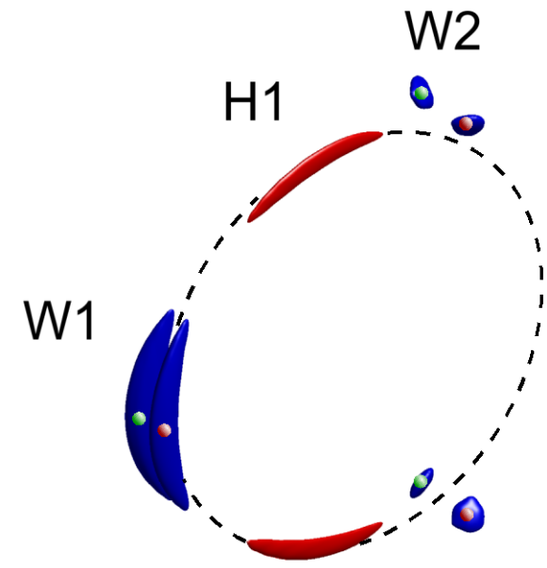

(c)

3 Fermi surfaces detected

First experimental evidence for separate Fermi surface pockets around W1 and W2 Weyl points

TaAs - band structure

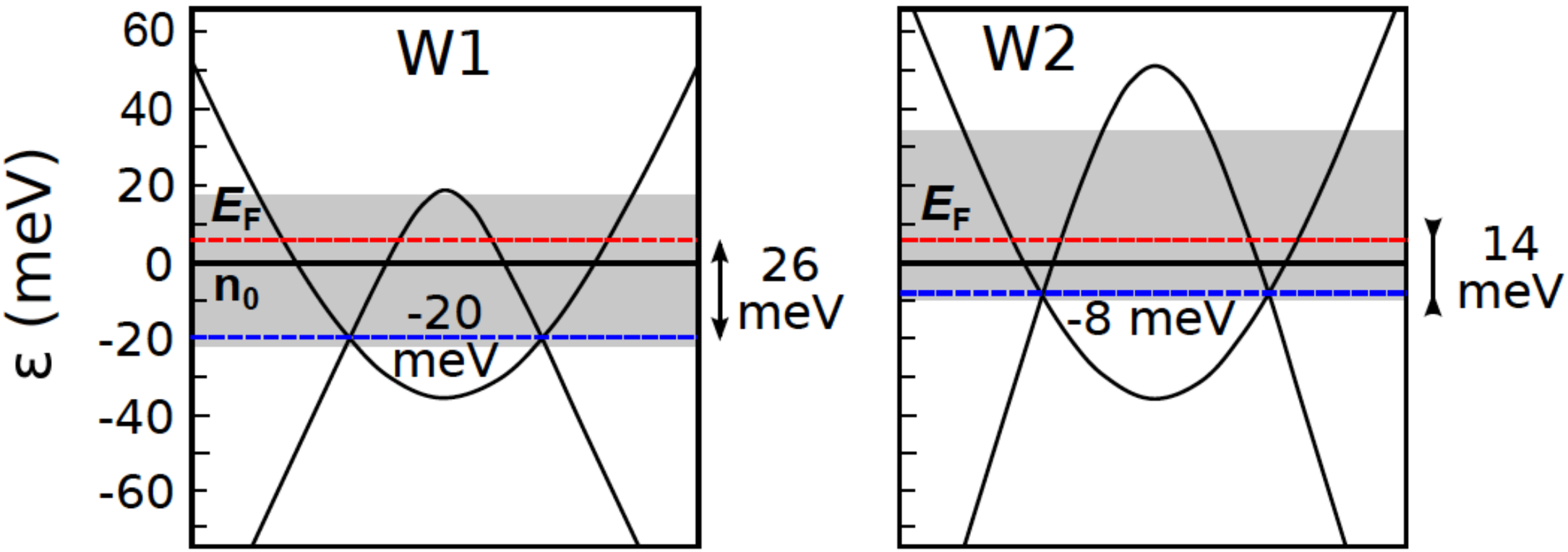

Overlap of energy range for independent FS pockets for W1 and W2

Chirality well defined

Band-resolved Berry phase

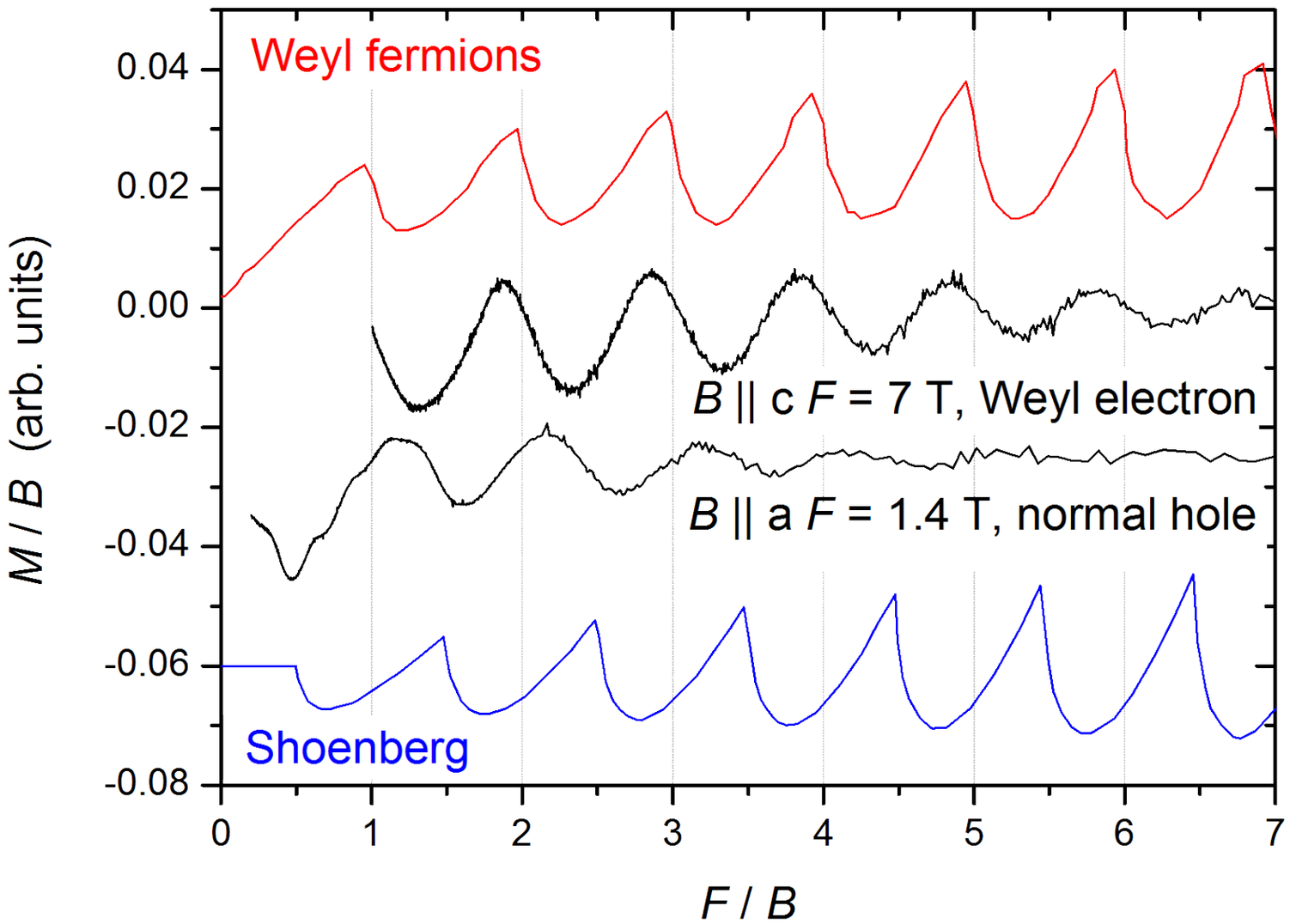

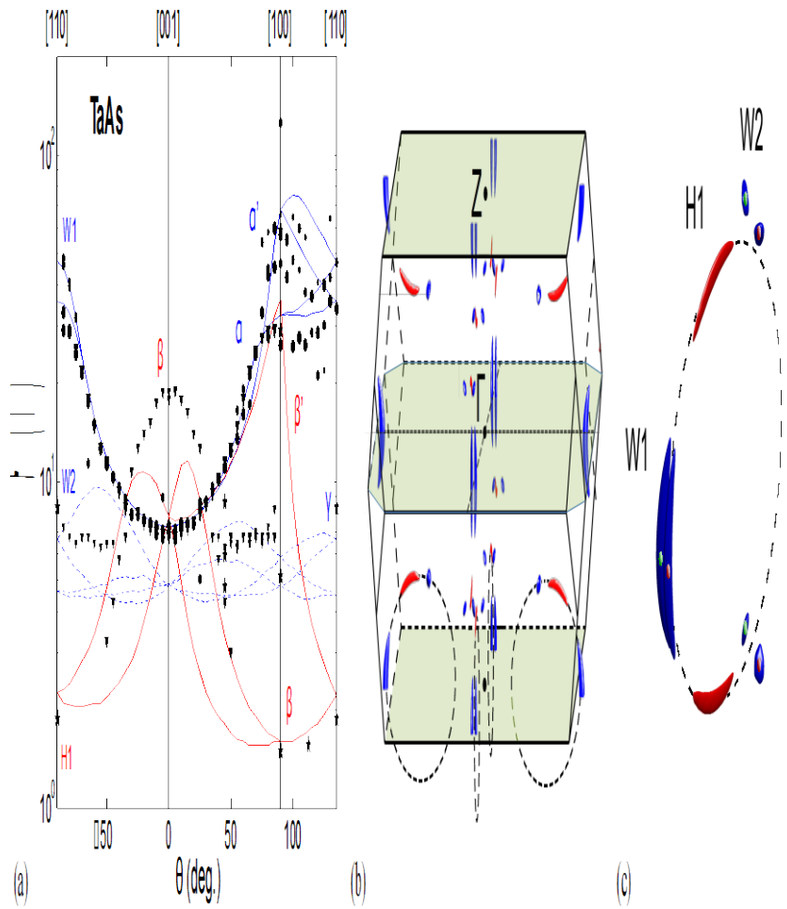

Phase shift between chiral and non-chiral oscillations

First thermodynamic evidence for Berry phase

Shoenberg book

Ashby, EPJ B, 2014

TaAs

- Independent Weyl pockets
- Well-defined chirality
- Weyl nodes close to the Fermi energy

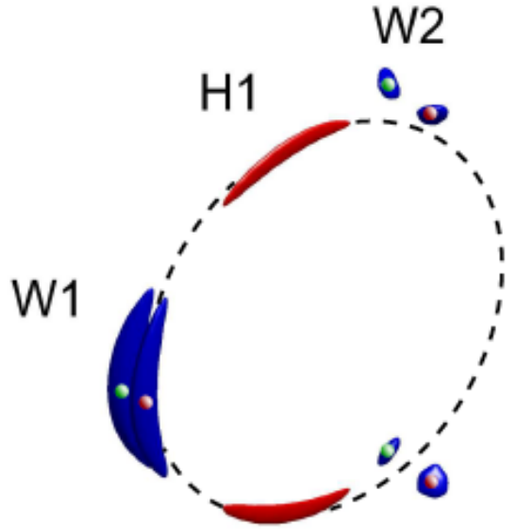

Arnold *et al.* PRL 2016

Summary

- TaP: Pairs of Weyl nodes embeddec in big Fermi surfaces

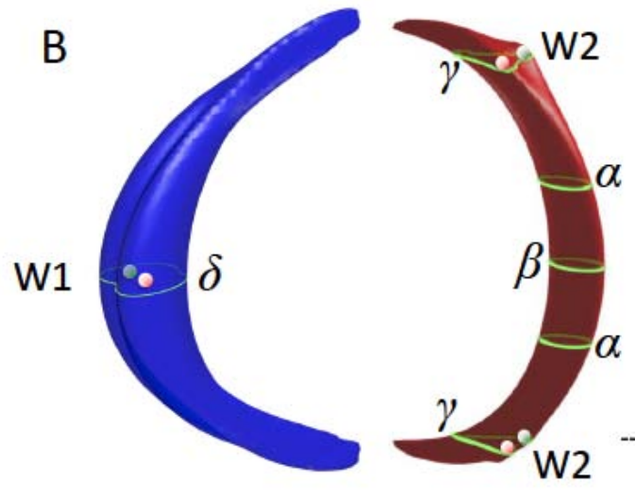

- TaAs: Separate Weyl pockets, well-defined chirality

- Berry phase in chiral pockets in TaAs

  Arnold *et al.* Nat. Comm. 2016
  Arnold *et al.* PRL 2016

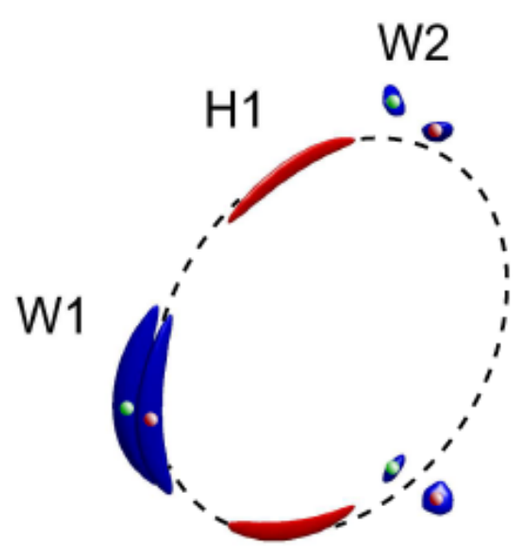

- Watch out for current jetting!

  Dos Reis et al. New J. Phys. 2016

Thank you for your attention!